Effect of Force-Constant Changes on the Incoherent Neutron Scattering from Cubic Crystals with Point Defects*

KATJA LAKATOS† AND J. A. KRUMHANSL
Laboratory of Atomic and Solid State Physics, Cornell University, Ithaca, New York 14850
(Received 18 April 1968)

This is a study of the vibrational properties of random substitutional impurities and their nearest neighbors in cubic monatomic harmonic crystals in the low-impurity-concentration limit. Mass changes, as well as force-constant changes between the impurity and its nearest and, in some cases, next-nearest neighbors, are taken into account. The problem is formulated in terms of an incoherent-neutron-scattering experiment, although the results are useful for other experiments as well. Analytic expressions are given for the resonance frequencies for all the normal modes of the defect cage in fcc and bcc lattices. Expressions for the mean-square displacement of the impurity and its nearest neighbors at all frequencies are given for the fcc case. Results are expressed in terms of perfect-lattice Green's functions. Numerical computations are performed on Al containing heavy impurities. The Al-impurity force constants are treated as parameters which are varied over a wide range.

I. INTRODUCTION

In recent years, much theoretical and experimental work has been done on the effects of impurities on lattice vibrations.[1–13] The theoretical work usually involves the evaluation of various lattice Green's functions or correlation functions that can be directly related to measurable quantities.

Most of the theory has been restricted to models in which only the mass of the impurities is assumed to be different from the host atoms.[1,2] Recently, some results have been obtained on the effects of force-constant changes between the impurities and their nearest neighbors with low impurity concentration.[3–10] Most of the work is restricted to special situations (e.g., equal central- and noncentral-force-constant changes, or only central-force-constant changes[11]) or to only one aspect of the problem (e.g., motion of the impurity only, not of other atoms in the lattice). Some of the work is restricted to finding the resonance or local-mode frequencies to determine such properties as the strength and width of the resonances.[9]

Many experimental techniques probe either the behavior of the impurities (e.g., optical absorption) or only the average behavior of the lattice (optical-absorption sidebands, thermal conductivity, heat capacity). By means of neutron-scattering experiments, however, it is possible to probe the various effects of impurities on lattice vibrations in a more detailed manner. With incoherent neutron scattering, one can directly measure the motion of the impurities and their neighbors, while coherent neutron scattering allows the study of the effect of impurities on individual phonons. Some coherent-neutron-scattering experiments have been performed.[12,13]

The object of this paper is to study the motion of impurities and their neighbors as a function of frequency at low concentrations in various cubic harmonic monatomic lattices. Force-constant changes between the impurities and their neighbors are taken into account, in addition to mass change. Resonance and local-mode conditions for the impurity and its neighbors are given for all the modes of the defect subsystem with arbitrary central- and noncentral-force-constant changes in fcc and bcc lattices. Expressions for the average-square displacement of the impurity and its neighbors as a function of frequency are given for the fcc case. The corresponding general results with central and noncentral force changes have also been found, but are too lengthy to be given explicitly here. Numerical results are given for Al containing heavy impurities. They show significant differences from the simple mass-defect case.

The problem is formulated in terms of an incoherent-neutron-scattering experiment, although the correlation functions found here are useful for other experiments as well. The effects of the impurities on the lattice phonons

* Support for this work was provided by the U. S. Atomic Energy Commission under Contract No. AT(30-1)-3699, Technical Report No. NYO-3699-32, and by the Advanced Research Projects Agency through the use of the Central Facilities of Materials Science Center, Report No. 1032, Cornell University. This paper is based on a thesis submitted by K. Lakatos in partial fulfillment of the requirements for the Ph.D. degree in Physics at Cornell University.

† Present address: Department of Physics and Astronomy, University of Rochester, Rochester, N. Y.

[1] P. G. Dawber and R. J. Elliott, Proc. Roy. Soc. (London) **273A**, 222 (1963). Refs. 1–3 contain many related references.
[2] D. W. Taylor, thesis, Oxford University, 1965 (unpublished).
[3] A. A. Maradudin, Rept. Progr. Phys. **28**, (1965).
[4] W. M. Visscher, Phys. Rev. **129**, 28 (1963).
[5] A. A. Maradudin, E. W. Montroll, and G. H. Weiss, in *Solid State Physics*, edited by F. Seitz and D. Turnbull (Academic Press Inc., New York, 1963), Suppl. 3.
[6] W. M. Hartmann and R. J. Elliott, Proc. Phys. Soc. (London) **91**, 187 (1967).
[7] H. C. Poon and A. Bienenstock, Phys. Rev. **152**, 718 (1966); **141**, 710 (1966).
[8] G. Benedek and G. F. Nardelli, Phys. Rev. **155**, 1004 (1967).
[9] S. N. Behera and B. Deo, Phys. Rev. **153**, 728 (1967).
[10] T. P. Martin, Phys. Rev. **160**, 686 (1967).
[11] While this manuscript was in preparation, a paper by Philip D. Mannheim appeared in Phys. Rev. **165**, 1011 (1968), which greatly simplifies impurity results for fcc and bcc lattices with nearest-neighbor central force constants among host atoms. We have made no such restrictions in the present calculations.
[12] E. C. Svensson and B. N. Brockhouse, Phys. Rev. Letters **18**, 858 (1967); E. C. Svensson, B. N. Brockhouse, and J. M. Rowe, Solid State Commun. **3**, 245 (1965).
[13] H. B. Møller and A. R. Mackintosh, Phys. Rev. Letters **15**, 623 (1965).

(e.g., shift, broadening, and branch mixing), measurable by coherent neutron scattering, have also been studied and will be presented in a subsequent paper.

II. THEORY

We treat the scattering of neutrons from the lattice in the usual Fermi pseudopotential or scattering-length approximation.[14–16] The single-phonon contribution to the scattering cross section from an harmonic lattice per unit solid angle per unit of outgoing energy per atom in the Born approximation is then given by (the $\hbar=1$ convention will be followed throughout)

$$\frac{d^2\sigma}{d\Omega d\omega}=\frac{1}{2\pi}\frac{|k_2|}{|k_1|}S(\mathbf{K},\omega), \tag{1}$$

where $\mathbf{k}_1$ is the incoming neutron momentum, $\mathbf{k}_2$ is the outgoing neutron momentum, $\omega=(k_2^2-k_1^2)/2m$, m is the neutron mass, $\mathbf{K}=\mathbf{k}_2-\mathbf{k}_1$, and

$$S(\mathbf{K},\omega)=\frac{1}{N}\sum_{l,l'}A_lA^*_{l'}e^{i\mathbf{K}\cdot(\mathbf{R}_l-\mathbf{R}_{l'})}\times\int_{-\infty}^{\infty}dt\,e^{i\omega t}\langle\mathbf{K}\cdot\mathbf{u}(l,t)\mathbf{K}\cdot\mathbf{u}(l',0)\rangle. \tag{2}$$

Here, $\mathbf{R}_l$ is the equilibrium position of atom l, $\mathbf{u}(l,t)$ is the instantaneous displacement of atom l from equilibrium, $A_l=a_l\exp\{-\frac{1}{2}\langle[\mathbf{K}\cdot\mathbf{u}(l)]^2\rangle\}$ is the thermalized scattering length, $\exp\{-\frac{1}{2}\langle[\mathbf{K}\cdot\mathbf{u}(l)]^2\rangle\}$ is the Debye-Waller factor, a_l is the complex scattering length of atom l, $\langle\theta\rangle=(\mathrm{Tr}e^{-\beta(H-\mu N)}\theta)/(\mathrm{Tr}e^{-\beta(H-\mu N)})$, and H is the full Hamiltonian of the system.

Let

$$A_l=a_{l\ \mathrm{eff}}e^{-\Delta} \tag{3}$$

define the temperature-dependent quantity $a_{l\ \mathrm{eff}}$,[2,15] where $e^{-\Delta}$ is the Debye-Waller factor for the perfect lattice.

We shall now make a major assumption, namely, that the solute atoms are distributed completely at random, with no chemical or other tendency to be correlated in position. Random variations in $a_{l\ \mathrm{eff}}$ as a function of lattice site l give rise to incoherent scattering. In the system under consideration here, there are two sources of incoherent scattering in addition to those already present in the perfect lattice: (a) The impurities usually have a different scattering length than the host atoms, and (b) the Debye-Waller factors of the impurities and those neighbors appreciably affected by them differ from that of a perfect-lattice atom.

Denoting the effective scattering length of impurity s by $b_{s\ \mathrm{eff}}$, of a nearest neighbor of an impurity by $f_{n\ \mathrm{eff}}$, and of host atom l by $a_{l\ \mathrm{eff}}$, we can write

$$a_{l\ \mathrm{eff}}=a^{\mathrm{coh}}+a^{\mathrm{inc}}e^{i\phi_l}, \tag{4}$$

where a^{coh} and a^{inc} are the true physical scattering lengths, and similarly for b and f; ϕ_l, ϕ_n, and ϕ_s are statistically independent random phases.

For use in the following equations we define

$$\langle\ \rangle_l\equiv\frac{1}{N-N_s-N_n}\sum_{l\neq n,s},$$
$$\langle\ \rangle_s\equiv\frac{1}{N_s}\sum_{s}, \tag{5}$$

and

$$\langle\ \rangle_n\equiv\frac{1}{N_n}\sum_{n}.$$

To zeroth order in impurity concentration, the average scattering length of the lattice is then

$$\langle a\rangle_l=a^{\mathrm{coh}}. \tag{6}$$

The sources of incoherent scattering are the deviations of the scattering lengths of the atoms from the average value. A proper calculation of the incoherent-scattering contribution has been done by Taylor[2] for the mass-defect case. However, it is difficult to generalize his method to the defect considered here. We define the incoherent contribution as that part of the scattering that is independent of scattering angle. Then to linear order in impurity concentration we obtain

$$\begin{aligned}d_{l\neq s,n}^2(T)&=\langle|a|^2\rangle_l-\langle a\rangle_l^2=(a^{\mathrm{inc}})^2,\\ d_s^2(T)&=\langle|b|^2\rangle_s-\langle b\rangle_s^2+\langle b-a\rangle_s^2\\ &=(b^{\mathrm{inc}})^2+(b^{\mathrm{coh}}-a^{\mathrm{coh}})^2,\\ d_n^2(T)&=(f^{\mathrm{inc}})^2+(f^{\mathrm{coh}}-a^{\mathrm{coh}})^2,\end{aligned} \tag{7a}$$

where

$$(N-N_s-N_n)d_{l\neq s,n}^2+N_sd_s^2+N_nd_n^2=N([\![A^2]\!]-[\![A]\!]^2),$$
$$[\![A^2]\!]=[(N-N_s-N_n)/N]\langle|a|^2\rangle_l+(N_s/N)\langle|b|^2\rangle_s+(N_n/N)\langle|f|^2\rangle_n, \tag{7b}$$
$$[\![A]\!]=[(N-N_s-N_n)/N]\langle a\rangle_l+(N_s/N)\langle b\rangle_s+(N_n/N)\langle f\rangle_n,$$

and only terms of order 1, N_s/N, and N_n/N are retained. The fact that the average scattering length of the impurities is $\langle b\rangle_s$ and that of their nearest neighbors is $\langle f\rangle_n$ rather than $\langle a\rangle_l$ has been accounted for. The source of the terms a^{inc}, b^{inc}, and f^{inc} is dynamical, while that of $b^{\mathrm{coh}}-a^{\mathrm{coh}}$ and $f^{\mathrm{coh}}-a^{\mathrm{coh}}$ is spatial, i.e., the positions of the impurities are random.

Equation (2) can now be separated into coherent

[14] L. S. Kothari and K. S. Singwi, in *Solid State Physics*, edited by F. Seitz and D. Turnbull (Academic Press Inc., New York, 1959), Vol. 8.

[15] A. Sjolander, in *Phonons and Phonon Interactions*, edited by T. A. Bak (W. A. Benjamin, Inc., New York, 1964).

[16] R. J. Elliott and A. A. Maradudin, in *Proceedings of the Chalk River Symposium on Inelastic Scattering of Neutrons Solids and Liquids* (International Atomic Energy Agency, Vienna, 1963), Vol. I, p. 231.

and incoherent contributions[2,15]:

$$S(\mathbf{K},\omega)=S_{\rm coh}(\mathbf{K},\omega)+S_{\rm inc}(\mathbf{K},\omega), \tag{8}$$

$$S_{\rm coh}(\mathbf{K},\omega)=e^{-2A}N^{-1}\langle a\rangle_l^2\sum_{l,l'}e^{i\mathbf{K}\cdot(\mathbf{R}_l-\mathbf{R}_{l'})}\times\int_{-\infty}^{\infty}dt\,e^{i\omega t}\langle\mathbf{K}\cdot\mathbf{u}(l,t)\mathbf{K}\cdot\mathbf{u}(l',0)\rangle, \tag{9}$$

and

$$S_{\rm inc}(\mathbf{K},\omega)=e^{-2A}N^{-1}\sum_l d_l^2(T)\times\int_{-\infty}^{\infty}dt\,e^{i\omega t}\langle\mathbf{K}\cdot\mathbf{u}(l,t)\mathbf{K}\cdot\mathbf{u}(l,0)\rangle. \tag{10}$$

The problem is reduced, as usual, to the evaluation of

$$\int_{-\infty}^{\infty}dt\,e^{i\omega t}\langle\mathbf{K}\cdot\mathbf{u}(l,t)\mathbf{K}\cdot\mathbf{u}(l',0)\rangle, \tag{11}$$

which can be done by the method of Green's functions.

To detect the behavior of the impurities in $S_{\rm inc}$ above the host-lattice background experimentally, the condition

$$cd_{\rm imp}^2\gg d_{\rm host}^2 \tag{12}$$

should be satisfied, where c is the impurity concentration. Some lower-bound estimates for c are given in Table I. We wish to call particular attention to the low concentrations of some impurities that may be studied. A general impression seems to have been created that incoherent scattering is not easily usable for the study of resonant modes. This is perhaps based on the erroneous assumption that an impurity with an *incoherent* cross section much larger than the host cross section is needed; Eq. (6) shows why this is not the case. The situation has been demonstrated experimentally by Chernoplekov[17] for Pb in Mg, in good agreement with estimates similar to those in Table I for Al alloys. We hope that the incoherent-scattering method may find more general use than it has so far.

For incoherent-neutron-scattering results presented in this paper, we only need Eq. (11) with $l=l'$. However, the general formulation is not more difficult and will provide a basis for the calculation of $S_{\rm coh}$ in a subsequent paper.

We assume low impurity concentration in the present discussions. The probability that two impurities are nearest or next-nearest neighbors, as well as the possibility of resonant scattering of excitations between defects, is assumed to be negligible. This treatment, therefore, does not consider the case of impurity clustering. Then only the single-impurity problem need be treated; at the end of the calculation, corrections are made that express results to linear order in impurity concentration. For the incoherent-scattering cross section this simply involves multiplying single-impurity effects by the number of impurities present.

TABLE I. Lower bound on impurity concentration for resonance-mode detection from incoherent neutron scattering.[a] Scattering lengths[b] in units of 10^{-12} cm.

Alloy	$a^{\rm coh}$	$\lvert a^{\rm inc}\rvert$	$b^{\rm coh}$	$\lvert b^{\rm inc}\rvert$	$c_{\rm LB}=d_{\rm host}^2/d_{\rm imp}^2$ (%)
Al(Au)	0.35	$\sim3\times10^{-2}$	0.76	0.37	~0.3
Al(Ag)	0.35	$\sim3\times10^{-2}$	0.61	0.39	~0.4
Al(Zn)	0.35	$\sim3\times10^{-2}$	0.59	0.09	~1.4
Al(Mn)	0.35	$\sim3\times10^{-2}$	−0.36	0.18	~0.2
Mg(Pb)	0.54	0.09	0.96	0.09	4.4
Be(Cu)	0.77	3×10^{-2}	0.79	0.23	1.4
Cu(W)	0.79	0.23	0.47	0.48	17
Ag(Hg)	0.61	0.39	1.3	0.60	18

[a] Solubility values are given in M. Hansen, *Constitution of Binary Alloys* (McGraw-Hill Book Co., New York, 1958), 2nd ed.; W. B. Pearson, *A Handbook of Lattice Spacings and Structures of Metals and Alloys* (The Macmillan Co., New York, 1958). Little information is available on solubility upon quenching.

[b] D. J. Hughes and J. A. Harvey, *Neutron Cross Sections* (McGraw-Hill Book Co., New York, 1955).

III. GREEN'S-FUNCTION FORMULATION

Equation (11) can be related to the retarded and advanced Green's functions defined by Zubarev[18] and used by Elliott and Taylor[19] for the mass-defect problem:

$$G_{\rm ret}(t,t')\equiv\ll A(t);B(t')\gg_r \equiv-i\langle[A(t);B(t')]\rangle\theta(t-t'), \tag{13a}$$

$$G_{\rm adv}(t,t')\equiv\ll A(t),B(t')\gg_a \equiv i\langle[A(t),B(t')]\rangle\theta(t'-t). \tag{13b}$$

Here, A and B are operators and

$$A(t)=e^{i(H-\mu N)t}Ae^{-i(H-\mu N)t},$$
$$[A,B]=AB-\eta BA,\quad \eta=\pm1$$
$$\theta(t)=1,\quad t>0$$
$$=0,\quad t<0.$$

η is $+1$ if A and B are Bose operators and -1 if they are Fermi operators. If they are neither or are mixed, either sign for η may be chosen. In our case, $\eta=1$. Both Green's functions satisfy the equation of motion

$$(i/2\pi)dG(t,t')/dt=\delta(t-t')\langle[A,B]\rangle+\ll[A,H];B\gg. \tag{14}$$

This equation is a direct consequence of the definition (13). The Green's functions are related to Eq. (11) by

$$\int_{-\infty}^{\infty}d(t-t')\,e^{i\omega(t-t')}\langle B(t')A(t)\rangle = \lim_{\delta\to0+}(e^{\beta\omega}-\eta)^{-1}[G(\omega+i\delta)-G(\omega-i\delta)], \tag{15}$$

[17] N. A. Chernoplekov and M. G. Zemlyanov, Zh. Eksperim. i Teor. Fiz. 49, 449 (1965)[English transl.: Soviet Phys.—JETP 22, 315 (1966)].

[18] D. N. Zubarev, Usp. Fiz. Nauk 71, 71 (1960) [English transl.: Soviet Phys.—Usp. 3, 320 (1960)].

[19] R. J. Elliott and D. W. Taylor, Proc. Phys. Soc. (London) 83, 189 (1964).

where

$$G(\omega\pm i\delta)=(2\pi)^{-1}\int_{-\infty}^{\infty}G(t-t')e^{i(\omega\pm i\delta)(t-t')}d(t-t'). \quad (16)$$

Here $G(t-t')=G_r$ with $+i\delta$ and G_a with $-i\delta$. Equation (15) incorporates the boundary condition necessary for the solution of Eq. (14).

The Green's functions needed here are

$$G_{im}(l,l';t-t')=2\pi\ll u_i(l,t);u_m(l',t')\gg, \quad (17)$$

where i and m denote Cartesian components. The Hamiltonian for the harmonic lattice containing impurities is

$$H=H_0+H', \quad (18)$$

where

$$H_0=\sum_l\frac{p_l^2}{2M_0}+\tfrac{1}{2}\sum_{\substack{i,m;\\ l,l'}}A_{im}(l,l')u_i(l)u_m(l') \quad (19)$$

and

$$H'=\sum_l\tfrac{1}{2}p_l^2\left(\frac{1}{M(l)}-\frac{1}{M_0}\right)+\tfrac{1}{2}\sum_{\substack{i,m;\\ l,l'}}[A_{im}'(l,l')-A_{im}(l,l')]u_i(l)u_m(l'). \quad (20)$$

H_0 is the perfect-lattice Hamiltonian with atomic mass M_0 and force constants $A_{im}(l,l')$. The only contributions to H' come from impurity sites and other atoms directly affected by force-constant changes. There is no restriction on the magnitude of the mass and force-constant changes.

In general, the equation of motion (14) for G introduces a new unknown Green's function that, in turn, has its own equation of motion. It is peculiar to a harmonic system that the original Green's function is recovered by taking two time derivatives. Fourier-transforming the resulting equation according to Eq. (16) gives

$$-M_0\omega^2G_{im}(l,l';\omega)+\sum_{l'',n}A_{in}(l,l'')G_{nm}(l'',l';\omega)=-\delta_{im}\delta(l,l')+\sum_{l'',n}Q_{in}(l,l'';\omega)G_{nm}(l'',l';\omega), \quad (21)$$

where

$$Q_{im}(l,l';\omega)=-[M_0-M(l)]\omega^2\delta_{im}\delta(l,l')+[A_{im}(l,l')-A_{im}'(l,l')] \quad (22)$$

contains all the information concerning the impurities. In Eqs. (21) and (22) and below, ω is complex unless otherwise indicated, or unless the imaginary part $i\delta$ is explicitly indicated.

The perfect-lattice solution of Eq. (22) ($Q=0$), denoted by G^0 and assumed to be known, is

$$G_{im}^0(l,l';\omega+i\delta)=(NM_0)^{-1}\times\sum_{\mathbf{k},\lambda}\frac{e_i(\mathbf{k},\lambda)e_m^*(\mathbf{k},\lambda)e^{i\mathbf{k}\cdot(\mathbf{R}_l-\mathbf{R}_{l'})}}{\omega^2-\omega^2(\mathbf{k},\lambda)+i\delta}, \quad (23)$$

where $e_i(\mathbf{k},\lambda)$ is the eigenvector component of the perfect lattice, $\omega(\mathbf{k},\lambda)$ are the eigenfrequencies, and λ is the branch index. Equation (21) can be reexpressed in terms of G^0. In matrix notation,

$$[-M_0\omega^2I+A]G=-I+QG \quad (24)$$

and

$$[-M_0\omega^2I+A]G^0=-I. \quad (25)$$

Therefore

$$G^0=-(-M_0\omega^2I+A)^{-1} \quad (26)$$

and

$$G=G^0+G^0QG, \quad (27)$$

or

$$G_{im}(l,l';\omega)=G_{im}^0(l,l';\omega)+M_0\epsilon\omega^2\sum_{s,n}G_{in}^0(l,s;\omega)G_{nm}(s,l';\omega)-\sum_{\substack{s_d,s_{d'};\\ n_1,n_2}}G_{in_1}^0(l,s_d;\omega)\Delta A_{n_1n_2}(s_d,s_{d'})G_{n_2m}(s_{d'},l';\omega). \quad (28)$$

Here $\epsilon=(M_0-M')/M_0$, M' is the impurity mass, s indicates impurity sites, s_d are the sites of atoms directly affected by force-constant changes, including the impurities, and

$$\Delta A_{im}(l,l')=A_{im}(l,l')-A_{im}'(l,l'). \quad (29)$$

Equation (29) can be rewritten in matrix notation in somewhat more detail than Eq. (28):

$$G=G^0+g^0Qg, \quad (30)$$

where G and G^0 have dimension $3N\times3N$, g and g^0 have dimension $3N\times3N_d$ or $3N_d\times3N$, and Q has dimension $3N_d\times3N_d$. N is the total number of atoms in the lattice and N_d is the number of atoms directly affected by force-constant changes. Letting l range over all the s_d in Eq. (28) gives

$$g=g^0+g_d^0Qg, \quad (31)$$

where g_d^0 has dimension $3N_d\times3N_d$, or

$$g=(1-g_d^0Q)^{-1}g^0. \quad (32)$$

The formal solution of Eq. (31) is then

$$G=G^0+g^0Q(1-g_d^0Q)^{-1}g^0 \quad (33)$$

or

$$G_{im}(l,l';\omega)=G_{im}^0(l,l';\omega)+\sum_{\substack{s_d,s_{d'},s_{d''};\\ n_1,n_2,n_3}}[G_{in_1}^0(l,s_d;\omega)Q_{n_1n_2}(s_d,s_{d'};\omega)\times(1-g_d^0Q)^{-1}{}_{n_2n_3}(s_{d'},s_{d''};\omega)G_{n_3m}^0(s_{d''},l';\omega)], \quad (34)$$

and the problem has been reduced to the evaluation of the inverse of the $3N_d\times3N_d$ matrix $1-g_d^0Q$.

IV. SOLUTION TO LINEAR ORDER IN IMPURITY CONCENTRATION

Consider a lattice with a single impurity. For an fcc lattice in which force-constant changes to nearest

neighbors are included, $N_d=13$. In a bcc lattice, next-nearest-neighbor force changes must also be considered, because their distance from the impurity is not much greater than that of the nearest neighbors: $N_d=15$.

To invert $1-g_d{}^0Q$ analytically, it is first necessary to block-diagonalize it using the symmetry properties of the lattice. Thus

$$(1-g_d{}^0Q)^{-1}=V^{-1}[V(1-g_d{}^0Q)V^{-1}]^{-1}V, \quad (35)$$

where $V(1-g_d{}^0Q)V^{-1}$ is block-diagonal and V is determined from the symmetry of the lattice. Each block in $[V(1-g_d{}^0Q)V^{-1}]^{-1}$ corresponds to a normal mode of the defect cage, and is of the form $1/D_\Gamma\times$(a submatrix), where the D_Γ are functions of frequency and the various parameter changes. They are the determinants that occur in the inversion. As will be seen below, resonances occur at frequencies satisfying $\mathrm{Re}D_\Gamma(\omega)\approx 0$. Explicit expressions for the D_Γ are given in Appendices A and B for the fcc and bcc cases, respectively. Results for general central- and noncentral-force-constant changes are given. We have complete analytic expressions for matrix $Q(1-g_d{}^0Q)^{-1}$ for fcc and $1-g_d{}^0Q$ for bcc lattices with central-force-constant changes, but the results are too lengthy to be included here.

A. Incoherent Scattering from Impurities

The incoherent-scattering contribution from the impurities themselves is related to

$$S_{\mathrm{inc}}(\omega,\mathrm{imp})=[e^{-2W}cd_{\mathrm{imp}}{}^2n(\omega)]\times[\lim_{\delta\to 0+}-\mathrm{Im}G_{ii}(0,0;\omega+i\omega)], \quad (36)$$

obtained from Eq. (34) by letting $l=l'=0$ be the impurity site [see Eqs. (11), (15), and (17)]. Here $n(\omega)=\cosh\omega/2k_BT$, and emission and absorption processes of frequency ω have been combined. $G_{i\neq m}(0,0)=0$ by the symmetry of the system. Only the Γ_{15} mode is considered, because it is the only mode in which the impurity moves. For subsequent comparison with the force-constant-change results, we first consider results for a perfect-lattice atom and for an impurity in the mass-defect approximation.[2,16,19] From Eq. (23) with $l=l'$ the former gives

$$\begin{aligned}
&-\mathrm{Im}G_{ii}{}^0(0,0,\omega+i\delta)\\
&=-\mathrm{Im}\frac{1}{3NM_0}\sum_{\mathbf{k},\lambda}\frac{1}{\omega^2-\omega^2(\mathbf{k},\lambda)+i\delta}\\
&=-\mathrm{Im}\int_0^\infty\frac{D(\omega')d\omega'}{\omega^2-\omega'^2+i\delta}\\
&=-\frac{1}{M_0}\mathrm{Im}\left(P\int_0^\infty\frac{D(\omega')d\omega'}{\omega^2-\omega'^2}d\omega'-\frac{1}{2}\frac{i\pi}{\omega}D(\omega)\right)\\
&=(\pi/2M_0)D(\omega)/\omega. \quad (37)
\end{aligned}$$

Here, P denotes the principal-value integral and $D(\omega)$ is the normalized density of states of the perfect lattice:

$$\int_0^\infty D(\omega)d\omega=1. \quad (38)$$

Thus, the square displacement or incoherent-scattering contribution from a perfect-lattice atom at a given frequency is proportional to the density of states at that frequency. In a defect lattice, the scattering from atoms that are not too close to the defects is also given approximately by Eq. (37).

In the mass-defect approximation, the impurity Green's function is given by

$$\begin{aligned}
&-\mathrm{Im}G_{ii}(0,0;\omega+i\delta)\\
&=-\mathrm{Im}\frac{G_{ii}{}^0(0,0;\omega+i\delta)}{1-M_0\epsilon\omega^2G_{ii}{}^0(0,0;\omega+i\delta)}\\
&=\frac{\pi}{2M_0}\frac{D(\omega)}{\omega}\Big/\left\{\left[1-\epsilon\omega^2P\int_0^\infty\frac{D(\omega')}{\omega^2-\omega'^2}d\omega'\right]^2+\tfrac{1}{4}\pi^2\omega^2\epsilon^2D^2(\omega)\right\}. \quad (39)
\end{aligned}$$

The impurity motion is thus that of a perfect-lattice atom modified by a "resonance denominator." The impurity amplitude or scattering is greatest at frequencies ω_0 that satisfy the conditions

$$\begin{aligned}
&(d/d\omega^2)[-\mathrm{Im}G_{ii}(0,0;\omega_0+i\delta)]=0\\
&\text{and}\\
&[d^2/(d\omega^2)^2][-\mathrm{Im}G_{ii}(0,0;\omega_0+i\delta)]<0, \quad (40)
\end{aligned}$$

or approximately when the "resonance condition"

$$\epsilon\omega_0{}^2P\int_0^\infty\frac{D(\omega')}{\omega_0{}^2-\omega'^2}d\omega'\simeq 1 \quad (41)$$

is satisfied. Note that although Eq. (41) is generally used as the resonance condition, the frequencies obtained from it can differ from those found through Eq. (40) by as much as $\sim 15\%$ in typical solids when the density of states $D(\omega_0)$ varies rapidly.

If ϵ is close to 1 (very light impurity), Eq. (41) may be satisfied for a frequency ω_L above the lattice band $[D(\omega_L)=0]$, giving rise to a localized mode

$$-\mathrm{Im}G_{ii}(0,0;\omega_L+i\delta)=\frac{1}{M_0\omega_L{}^2\epsilon}\delta\left(1-\epsilon\omega_L{}^2\int_0^\infty\frac{D(\omega')d\omega'}{\omega_L{}^2-\omega'^2}\right). \quad (42)$$

If ϵ is large and negative (heavy impurity), Eq. (41) may be satisfied at a frequency ω_0 within the lattice band, giving rise to a resonance mode. Equation (39) is then similar to a Lorentzian, and the quantity $\frac{1}{2}\pi\omega_0\epsilon D(\omega_0)$

is roughly the width of the resonance or inverse lifetime for an excitation of frequency ω_0 to remain localized at the impurity.

In the presence of force-constant changes the resonance characteristics of the impurity involve perfect-lattice Green's functions other than $G_{ii}^0(0,0)$. This is a consequence of the fact that the defect is no longer a point imperfection. Let $G_{ij}^0(l,l';\omega+i\delta)\equiv G_{ij}^0(n_1,n_2,n_3)$, where $(n_1,n_2,n_3)a=\mathbf{R}_l-\mathbf{R}_{l'}$, and $2a$ is the unit-cube edge. For the fcc lattice, there is a total of 702 possible perfect-lattice Green's functions among the impurity and its 12 nearest neighbors. By symmetry considerations, only 13 of these are independent. For the bcc lattice, including nearest and next-nearest neighbors of the impurity, of the 1980 Green's functions 15 are independent. The fcc and bcc Green's functions are given in Table II.

When only central-force-constant changes are considered, the impurity Green's function in the fcc lattice, using the symbols of Table II and the definition of α of Appendix A, is

$$\begin{aligned} &G_{ii}(0,0;\omega+i\delta)\\ &\quad=G_{\rm eff}/[1-M_0\epsilon\omega^2G_{\rm eff}+2\alpha(G_1-8G_2-8G_4+X)],\\ &\qquad G_{\rm eff}=G_1+2\alpha[G_1{}^2-4(G_2+G_4)^2+G_1X],\\ &\qquad X=G_3-G_4+G_7+G_9+G_{10}+2G_{12}+G_{13}. \end{aligned} \tag{43}$$

We have also evaluated the impurity Green's function for general central- and noncentral-force-constant changes, but the result is too lengthy and unrevealing to be reproduced here. As in the mass-change case, resonance or localized modes occur when Eqs. (40) are satisfied, or approximately when the real part of the denominator of Eq. (43) is zero for some frequency. The resonance condition is thus bilinear in mass and force-constant change. It cannot be factored into a mass- and force-constant-dependent terms: Every resonance is determined by both, although one or the other might dominate the properties of a particular resonance. If noncentral-force-constant changes are included, the resonance condition is a quadrilinear function in the defect parameters.

TABLE II. Perfect-lattice Green's functions for fcc and bcc cases.

Symbol	fcc	bcc
G_1	$G_{ii}^0(0,0,0)$	$G_{ii}^0(0,0,0)$
G_2	$G_{xx}^0(1,1,0)$	$G_{xx}^0(1,1,1)$
G_3	$G_{zz}^0(1,1,0)$	$G_{xy}^0(1,1,1)$
G_4	$G_{xy}^0(1,1,0)$	$G_{xx}^0(2,-2,0)$
G_5	$G_{xx}^0(0,0,2)$	$G_{zz}^0(2,-2,0)$
G_6	$G_{zz}^0(0,0,2)$	$G_{xy}^0(2,-2,0)$
G_7	$G_{xx}^0(2,2,0)$	$G_{xx}^0(2,2,2)$
G_8	$G_{zz}^0(2,2,0)$	$G_{xy}^0(2,2,2)$
G_9	$G_{xy}^0(2,2,0)$	$G_{xx}^0(2,0,0)$
G_{10}	$G_{xx}^0(2,1,1)$	$G_{yy}^0(2,0,0)$
G_{11}	$G_{yy}^0(2,1,1)$	$G_{xx}^0(4,0,0)$
G_{12}	$G_{xy}^0(2,1,1)$	$G_{yy}^0(4,0,0)$
G_{13}	$G_{yz}^0(2,1,1)$	$G_{xx}^0(3,1,1)$
G_{14}		$G_{yy}^0(3,1,1)$
G_{15}		$G_{xy}^0(3,1,1)$
G_{16}		$G_{yz}^0(3,1,1)$

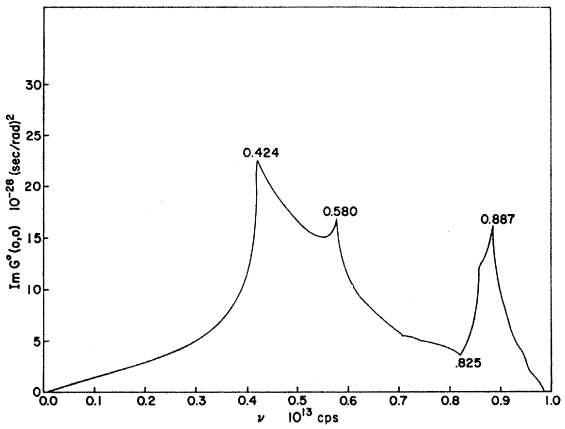

FIG. 1. Im$G^0(0,0,0)$ for Al perfect lattice from experimental data of Oak Ridge National Laboratories (Ref. 23).

We have evaluated Im$G_{ii}(0,0;\omega+i\delta)$ for heavy impurities with several mass and force-constant changes in Al. Pure Al is a very weak incoherent scatterer, so that defect characteristics should be easily observable. Accurate Al data were supplied to us by Raubenheimer and Gilat[20] of Oak Ridge National Laboratories. They also made available to us a very accurate method to calculate frequency spectra from experimentally determined perfect-lattice force constants.[21] We have used a slightly modified version of their method to evaluate the various perfect-lattice Green's functions.

Figure 1 shows Im$G^0(0,0,0)$ for Al, given by Eq. (37). Figure 2 shows Im$G(0,0,\omega)$ for Au ($\epsilon=-6.3017$), Ag ($\epsilon=-2.9983$), Zn ($\epsilon=-1.4233$), and Mn ($\epsilon=-1.0363$) in Al in the mass-defect approximation, Eq. (39). The

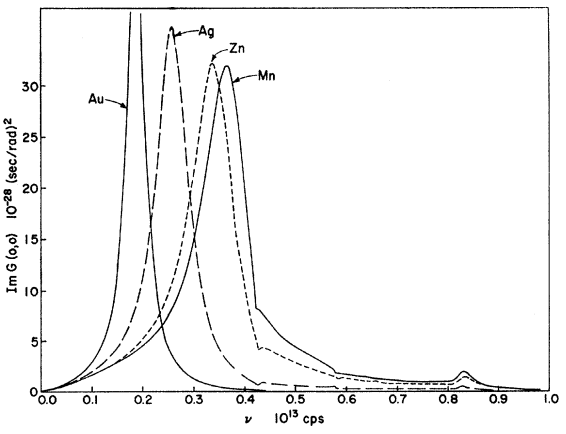

FIG. 2. Impurity Green's function for Au, Ag, Zn, and Mn in Al in the mass-defect approximation.

[20] L. J. Raubenheimer and G. Gilat (private communication).
[21] L. J. Raubenheimer and G. Gilat, Oak Ridge National Laboratory Report No. ORNL-TM-1425, 1966 (unpublished).

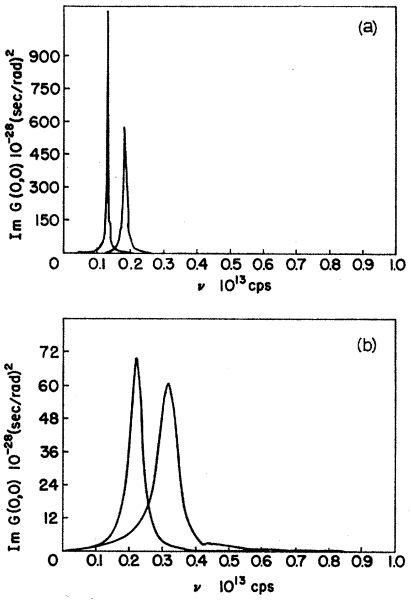

FIG. 3. Impurity Green's function with mass and central-force-constant changes: (a) Ag in Al, with central-force constants 70 (high peak) and 30% *weaker* than in the host lattice; (b) similarly for Mn in Al.

low-frequency resonance becomes stronger and narrower as the mass of the impurity increases and the resonance frequency decreases.

As the impurity mass decreases in Fig. 2, a small peaked structure begins to appear in the high-frequency region where the perfect-Al-lattice density of states has a minimum. Equation (40) can be satisfied, or almost satisfied, for high ω_0 even for negative ϵ, if the principal-

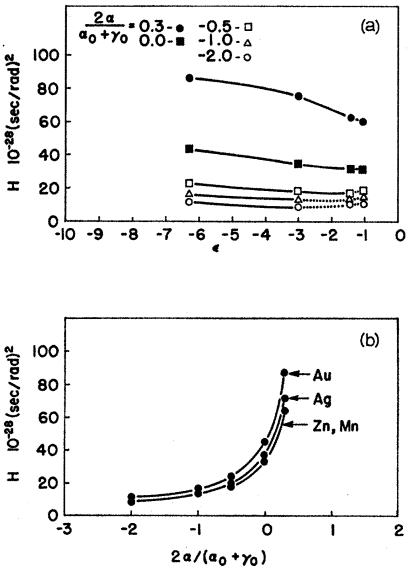

FIG. 4. Height of the impurity-resonance peak in ImG(0,0,0) as a function of (a) mass change for several central-force-constant changes; (b) central-force-constant changes for several mass changes.

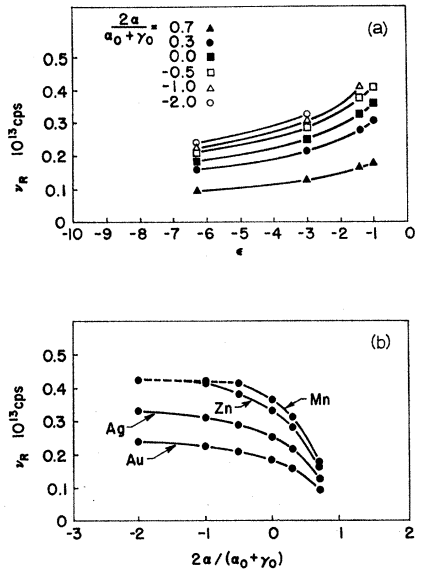

FIG. 5. Impurity resonance frequency as a function of (a) mass change for several central-force-constant changes; (b) central-force-constant change for several mass changes.

value integral, whose largest contributions come from the region D ($\omega' \sim \omega_0$), is sufficiently small and negative. The host lattice is unable to propagate excitations of this frequency effectively and they tend to remain spatially and energetically localized at the impurity.

Figure 3 shows the effect of 70 and 30% weaker central force constants for impurities with the masses of Ag and Mn in Al, Eq. (43) (note scale changes). The weakening of force constants for fixed ϵ drastically sharpens and strengthens the resonance peak and lowers the resonance frequency. The effects of weakening force constants are much stronger than those of a mass increase, as shown in Figs. 4 and 5. Lower resonance frequencies can be reached with weakly bound impurities even if the latter are light than by just increasing the impurity mass.

Note that in the heavy-mass–weak-force cases there is still only one low-frequency resonance, even though more parameters have now been varied. We shall deal briefly with the case of central and noncentral force-constant changes later.

In general, the situation in which mass and forces change in opposite directions is more interesting than when they change in the same direction. We have studied the case of heavy impurities with strong forces. Figures 6–8 show ImG_{ii}(0,0,ω) for impurities with the masses of Ag, Mn, and Al in Al for central-force constants 50, 100, and 200% stronger than in the host lattice. In the $\epsilon<0$ cases there is still a low-frequency resonance mode that moves up in frequency and loses strength and sharpness with increasing force constant. This behavior continues until the absolute fractional change in force constant $|\Delta A/A| \approx |\epsilon|$, when the mass and force effects in the low portion of the band tend to

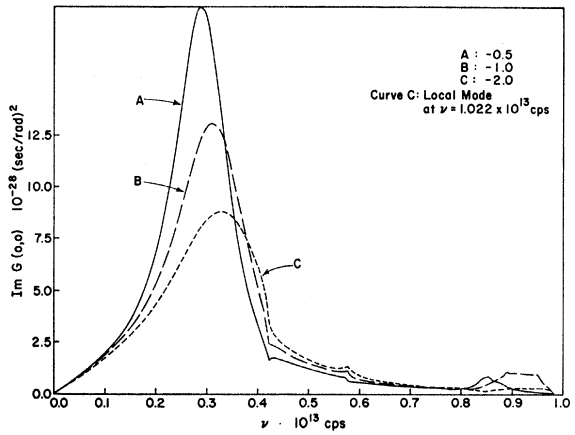

FIG. 6. Impurity Green's function for Ag in Al with mass and central force-constant changes. Curves A, B, and C correspond to forces that are 50, 100, and 200% *stronger* than in the host lattice, respectively. A high-frequency local mode appears in case C.

cancel and the perfect-lattice characteristics begin to reappear. The low-resonance peak then coincides with the first maximum in the host-lattice density of states, and a rather drastic mass or force change is needed to move it. This reflects the fact that the eigenstates of the system depend on the sum of potential and kinetic energies. In any lattice that itself scatterers incoherently, the effect of adding impurities with such a combination of mass and force changes would hardly be discernible in the low portion of the frequency spectrum.

The increase in force constants has a strong effect in the high-frequency portion of the spectrum. As the forces become stronger, the peaked structure that began to appear in Fig. 2 becomes enhanced and pushed to higher frequencies until it becomes a localized mode. As the resonance frequency increases within the band, the peak is broadened, because it approaches the maximum in the perfect-lattice density of states: The host lattice can easily propagate excitations at these frequencies and they have a short lifetime at the impurity. Beyond the maximum the resonance peak again becomes sharper until it becomes a very sharp localized mode. The upper end of the curve in Fig. 7, which has a resonance peak almost at the band edge, has been indicated by a dotted line because in this region our calculations are very sensitive to small errors, and the amplitude indicated may be quite inaccurate.

As the impurity mass increases, the force-constant change needed for a localized mode to appear also increases, but it is difficult to give an exact criterion other than Eq. (43) for the ratio $\Delta M/\Delta A$ needed. The fractional mass and force changes must be roughly equal and opposite.

Table III is a summary of the central-force-constant-change results for various mass changes. As resonance peaks approach peaks in the perfect-lattice spectrum, the width at half-height does not have much meaning because of the asymmetry of the curves, so that they are not indicated. The height of the very narrowest resonances is inaccurate because computations were made at discrete intervals of $\Delta\nu = 0.002 \times 10^{13}$ cps. Localized modes are followed by a letter L.

Table IV shows the impurity Einstein-oscillator frequencies for the various mass and central force-constant changes considered.[22] The agreement between this value and that of the actual low-frequency resonance, indicated in parentheses, is remarkably good when force constants are weaker than those of the perfect lattice. The impurity acts like an independent oscillator when it is weakly coupled to the lattice. As might be expected, the agreement is poor when force constants are stronger, and a simple Einstein-oscillator model cannot, of course, produce two resonance frequencies. A good estimate of the resonance and local-mode frequencies in this case

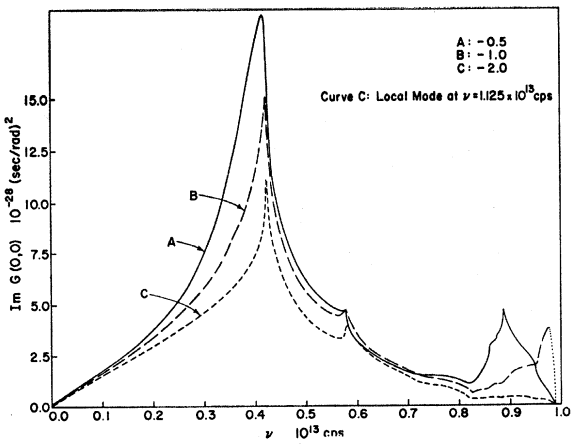

FIG. 7. Impurity Green's function for Mn in Al with mass and central force-constant changes. Curves A, B, and C correspond to forces that are 50, 100, and 200% *stronger* than in the host lattices, respectively. A high-frequency local mode appears in case C.

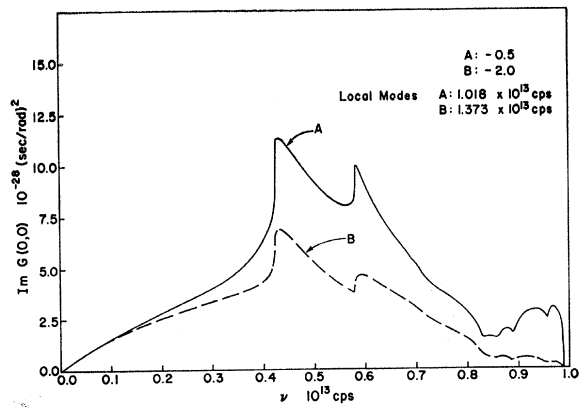

FIG. 8. Impurity Green's function for a defect with no mass change but with central force-constant changes in Al. Curves A and B correspond to forces which are 50 and 200% *stronger* than in the host lattice, respectively. High-frequency local modes appear in both cases.

[22] J. A. Krumhansl, in *Localized Excitations in Solids*, edited by R. F. Wallis (Plenum Press, Inc., New York, 1968).

TABLE III. Motion of impurities—central force-constant changes.

ϵ	$\Delta A/A$	Low-frequency resonance (10^{13} cps)	Width of resonance (10^{13} cps)	Height of resonance [10^{-28} (sec/rad)^2]	High-frequency resonance or local mode (10^{13} cps)
−6.3017 (Au)	−2	0.241	0.141	10.95	0.979
−6.3017	−1	0.225	0.102	16.21	∼0.887
−6.3017	−0.5	0.211	0.077	23.14	∼0.840
−6.3017	0	0.185	0.045	43.48	
−6.3017	0.3	0.161	0.026	85.93	
−6.3017	0.7	0.095	<0.010	>850	
−2.9983 (Ag)	−2	0.331	0.218	8.855	1.022 (L)
−2.9983	−1	0.311	0.166	13.09	∼0.9
−2.9983	−0.5	0.289	0.126	18.78	∼0.857
−2.9983	0	0.255	0.080	35.6	∼0.825
−2.9983	0.3	0.219	0.044	70.59	
−2.9983	0.7	0.131	<0.010	>1107	
−1.4233 (Zn)	−2	0.423		10.57	1.089 (L)
−1.4233	−1	0.417	0.152	13.40	0.983
−1.4233	−0.5	0.383	0.135	17.49	0.887
−1.4233	0	0.333	0.102	32.00	∼0.829
−1.4233	0.3	0.285	0.061	62.78	
−1.4233	0.7	0.167	<0.015	>586	
−1.0363 (Mn)	−2	0.423		11.21	1.125 (L)
−1.0363	−1	0.421		15.06	0.975
−1.0363	−0.5	0.417	0.118	19.10	0.889
−1.0363	0	0.367	0.104	31.85	0.833
−1.0363	0.3	0.313	0.067	61.41	
−1.0363	0.7	0.181	<0.015	>581	
0	−2				1.373 (L)
0	−1				1.142 (L)
0	−0.5				1.018 (L)

could probably be obtained by considering the impurity and its neighbors as a molecule embedded in a static lattice. Even the simplest version of the force-constant-change problem when forces are strong is far more complicated than the mass-defect case.

In the cases considered here, the results with both central and noncentral force changes are similar in character to those with only central force changes. The number of resonance and localized modes in the various cases does not change. This may, in part, be due to the fact that we have kept the relative magnitudes $|A_{\text{noncentral}}/A_{\text{central}}|$ equal to their relative magnitude in pure Al, where the ratio is ≈ 0.12.[20] Some results for the resonance in the low-frequency portion of the spectrum are given in Table V as a function of mass and central force-constant changes. Case 1 corresponds to either strengthening or weakening both central and weakening the noncentral force-constant changes, or vice versa. Case 3 corresponds to central force-constant changes only. Greater differences and perhaps more resonances would occur if the central and noncentral force-constant changes were more nearly equal in magnitude.

B. Incoherent Scattering from Nearest Neighbors of Impurity

A typical nearest-neighbor contribution to the scattering cross section is

$$S_{\text{inc}}(\omega,\ \text{neighbor}) = e^{-2\Delta} c d_{\text{nbr}}{}^2 n(\omega) \times \lim_{\delta\to 0} \sum_{i,m} K_i K_m \operatorname{Im} G_{im}(1,1;\omega+i\delta). \quad (44)$$

Here, $l=l'=1$ represents the nearest neighbor (1,1,0) and

$$G_{im}(1,1;\omega) = G_{ii}{}^0(0,0;\omega)\delta_{im} + \sum_{\substack{s_d,s_{d'};\\ n_1,n_2}} \{G_{in_1}{}^0(1,s_d;\omega)[Q(1-g_d{}^0Q)^{-1}]_{n_1n_2}(s_d,s_{d'};\omega) \times G_{n_2m}{}^0(s_{d'},1;\omega)\}. \quad (45)$$

TABLE IV. Einstein-oscillator frequencies versus computed resonances (in parentheses) in units of 10^{13} cps. $\nu_E = (4\alpha_{\text{new}}/4\pi^2 M)^{1/2}$.

ϵ \ $\Delta A/A$	−2	−1	−0.5	0	0.3	0.7
−6.3017 (Au)	0.317 (0.241)	0.259 (0.225)	0.225 (0.211)	0.183 (0.185)	0.153 (0.161)	0.100 (0.095)
−2.9983 (Ag)	0.427 (0.331)	0.350 (0.311)	0.303 (0.289)	0.248 (0.255)	0.207 (0.219)	0.136 (0.131)
−1.4233 (Zn)	0.548 (0.423)	0.448 (0.417)	0.388 (0.383)	0.317 (0.333)	0.265 (0.285)	0.173 (0.167)
−1.0363 (Mn)	0.597 (0.423)	0.489 (0.421)	0.424 (0.417)	0.345 (0.367)	0.288 (0.313)	0.190 (0.181)
0 (No mass change)	0.855	0.697	0.606	0.494	0.413	0.270

TABLE V. Motion of impurity—central and noncentral force-constant changes.

		Case 1			Case 2			Case 3		
ϵ	$\Delta A/A$ central	Low-frequency resonance (10^{13} cps)	Width (10^{13} cps)	Height [10^{-28} (sec/rad)^2]	Low-frequency resonance (10^{13} cps)	Width (10^{13} cps)	Height [10^{-28} (sec/rad)^2]	Low-frequency resonance (10^{13} cps)	Width (10^{13} cps)	Height [10^{-28} (sec/rad)^2]
−6.3017	−1	0.213	0.082	20.45	0.233	0.122	13.26	0.225	0.102	16.21
−6.3017	0	0.185	0.045	43.48	0.185	0.045	43.48	0.185	0.045	43.48
−6.3017	0.3	0.155	0.022	104.7	0.167	0.030	73.18	0.161	0.026	85.93
−6.3017	0.7	0.121	0.009	>333	0.059	···	···	0.095	<0.01	>850
−2.9983	−1	0.291	0.130	16.87	0.327	0.205	10.46	0.311	0.166	13.08
−2.9983	0	0.255	0.080	35.6	0.255	0.080	35.6	0.255	0.080	35.6
−2.9983	0.3	0.229	0.050	59.2	0.211	0.038	85.33	0.219	0.044	70.59
−2.9983	0.7	0.165	0.017	255.4	0.079	···	···	0.131	<0.005	>1107
−1.4233	−1	0.377	0.137	16.08	0.423	∼0.160	12.19	0.417	∼0.152	13.40
−1.4233	0	0.333	0.102	32.0	0.333	0.102	32.0	0.333	0.102	32.0
−1.4233	0.3	0.299	0.070	53.32	0.271	0.053	75.12	0.285	0.061	62.78
−1.4233	0.7	0.213	0.018	261.8	0.103	···	···	0.167	<0.015	>586
−1.0363	−1	0.406	0.116	16.99	0.423	∼0.166	11.52	0.421	∼0.177	15.06
−1.0363	0	0.367	0.104	31.85	0.367	0.104	31.85	0.367	0.104	31.85
−1.0363	0.3	0.331	0.080	52.30	0.299	0.059	72.69	0.313	0.067	61.41
−1.0363	0.7	0.233	0.025	235.9	0.115	···	···	0.181	<0.015	>581

By symmetry, only three independent Green's functions enter in Eq. (43), namely, Im$G_{xx}(1,1)$, Im$G_{zz}(1,1)$, and Im$G_{xy}(1,1)$. They are plotted separately below, since the combination in which they contribute to S_{inc} depends on **K**. Note that in the perfect lattice $G_{xx}(1,1) = G_{zz}(1,1)$ and $G_{xy}(1,1)=0$. Analytic expressions for $G_{im}(1,1)$ are given in Appendix C for the mass-defect and mass- and central-force-constant-change cases.

Mass-defect results are given first for comparison. The scale is here again the same as in Figs. 1 and 2. Figures 9 and 10 show Im$G_{im}(1,1)$ for the nearest neighbors of Ag and Mn in Al. The motion of the neighbors is very similar to that of an atom in the perfect lattice (Fig. 1). The perfect-lattice singularities all appear at exactly the same frequencies but are not as sharp here. The decrease in sharpness is not very sensitive to the value of ϵ as long as it is negative. The great decrease of the perfect-lattice peak at $\nu=0.580\times10^{13}$ cps in Im$G_{zz}(1,1)$ occurs for all negative ϵ and is difficult to explain. Im$G_{xy}(1,1)$ remains quite small in all cases. As $|\epsilon|$ increases, a remnant of the impurity resonance begins to appear in the motion of the neighbors. As seen in Fig. 9, this effect is absent for Mn in Al, while Im$G_{xx}(1,1)$ for Ag shows a considerable broad peak centered at $\nu=0.233\times10^{13}$ cps (ν resonance$=0.255\times10^{13}$ cps) and Im$G_{zz}(1,1)$ shows a broad peak around $\nu=0.221\times10^{13}$ cps.

In the mass-defect approximation, then, the drastic

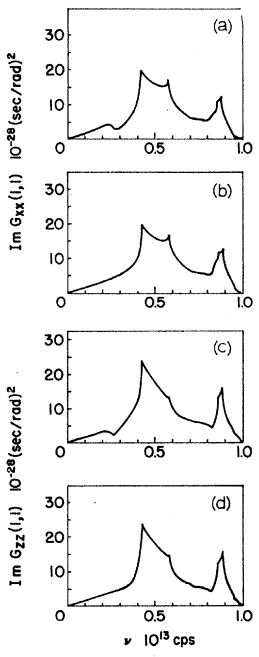

FIG. 9. Diagonal Green's functions for nearest neighbor (1,1,0) of impurities in Al in the mass-defect approximation: (a) ImG_{xx} for neighbor of Ag in Al; (b) ImG_{xx} for neighbor of Mn in Al; (c) ImG_{zz} for neighbor of Ag in Al; and (d) ImG_{zz} for neighbor of Mn in Al.

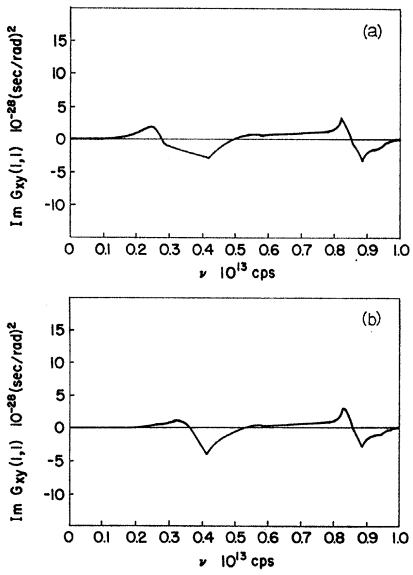

FIG. 10. Off-diagonal Green's functions for neighbor (1,1,0) of impurities in Al in the mass-defect approximation: (a) ImG_{xy} for neighbor of Ag in Al; (b) ImG_{xy} for neighbor of Mn in Al.

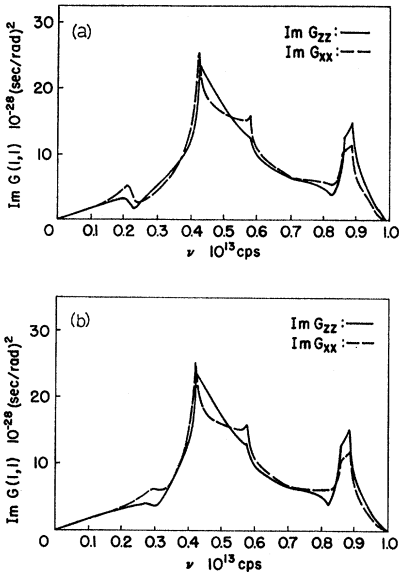

FIG. 11. Diagonal Green's functions for neighbor (1,1,0) of impurities in Al with mass changes and central force constants 70% *weaker* than in the host lattice: (a) neighbor of Ag in Al; (b) neighbor of Mn in Al.

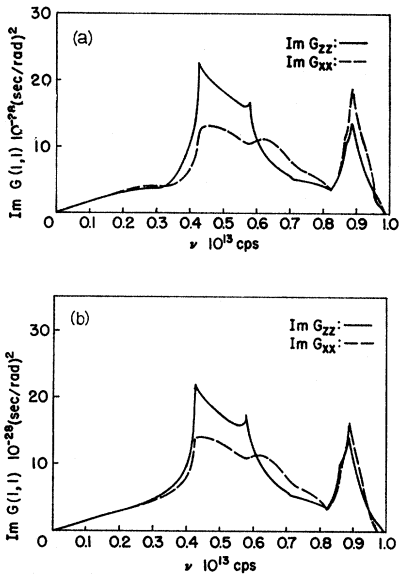

FIG. 13. Diagonal Green's functions for neighbor (1,1,0) of impurities in Al with mass changes and central-force constants 100% *stronger* than in the host lattice: (a) neighbor of Ag in Al; (b) neighbor of Mn in Al.

changes in S_{inc} occur at the impurity. The motion of its nearest neighbors is already very similar to that of a perfect-lattice atom.

Figures 11–14 show $\text{Im}G_{im}(1,1)$ for the nearest neighbors of impurities with the masses of Ag and Mn in Al for various central-force constant changes. In all cases, $\text{Im}G_{xx}$ is affected much more than $\text{Im}G_{zz}$, because the former represents motion along the force-constant-change direction (recall that $G_{yy}=G_{xx}$), while the latter represents motion perpendicular to the force change. We return to G_{zz} later.

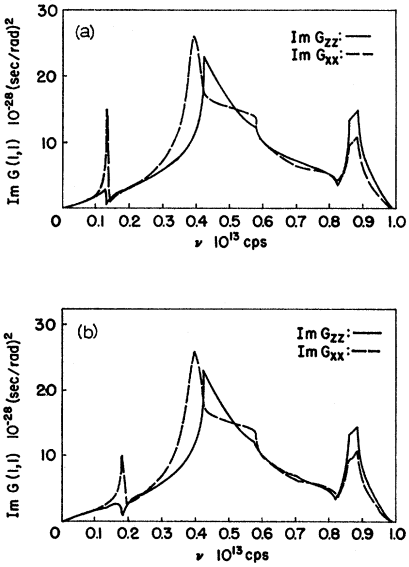

FIG. 12. Diagonal Green's functions for neighbor (1,1,0) of impurities in Al with mass changes and central force constants 30% *weaker* than in the host lattice: (a) neighbor of Ag in Al; (b) neighbor of Mn in Al.

When force constants are stronger, Fig. 13 shows that the high-frequency peaks are enhanced and the low-frequency ones washed out with respect to the perfect lattice, Fig. 1. The opposite occurs for weaker forces. The frequencies of the peaks are also shifted up (stronger forces) or down (weaker forces).

When forces are weak, the neighbors show a sharp low-frequency resonance in the neighborhood of the impurity resonance, much more pronounced than in

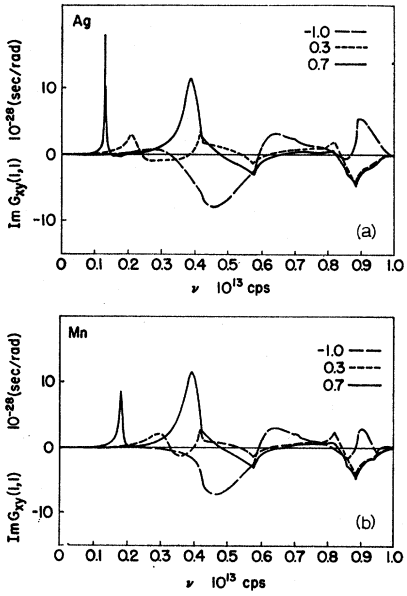

FIG. 14. Off-diagonal Green's functions for neighbor (1,1,0) of impurities in Al with central-force constants 70 and 30% *weaker* and 100% *stronger* than in the host lattice: (a) neighbor of Ag in Al; (b) neighbor of Mn in Al.

the mass-defect case. This does not contradict the earlier statement that in the weak-force case the impurity could be considered as being an Einstein oscillator in a static lattice: The impurity resonance amplitude increases far more rapidly with weakening forces than that of its neighbors.

In the cases considered here, localized modes of the impurity are caused by strong forces rather than by a light impurity mass. Since the nearest neighbors are directly coupled to the force changes, each one will vibrate at the local-mode frequencies with an amplitude roughly $\frac{1}{12}$ that of the impurity, which is connected to 12 strong force constants. A very sharp amplitude reduction occurs from next-nearest neighbors on.

In the cases considered here, the resonance behavior of the neighbors still comes only from the Γ_{15} mode even though $G_{im}(1,1)$ depends on all the modes of the cage. In fact, none of the other resonance denominators (Appendix A) even comes close to satisfying the resonance condition $\mathrm{Re}D=0$. Much larger force-constant changes are needed to observe resonances or local modes caused by them. In our calculations, the effect of the other modes is just to shift the Γ_{15} low-frequency peak down or up with respect to the impurity peak when the forces are weak or strong, respectively. When the central-force change is large (e.g., 70% weakening), $\mathrm{Im}G_{ii}(0,0)$ and $\mathrm{Im}G_{xx}(1,1)$ show a resonance at the same frequency, indicating that the Γ_{15} mode is then practically the only one of any importance in determining the peak frequency.

Note that the reason why the Γ_{15} mode shows resonance or local-mode characteristics for parameters for which the other modes do not is definitely *not* the fact that it alone depends on the mass change. This can be seen from Fig. 8: Even when there is no mass change, a 50% increase in force constants is already sufficient to give a Γ_{15} local mode. It is rather that the impurity, which moves only in the Γ_{15} mode, is affected by 12 force changes, so that the effective disturbance for this mode is much larger than for the others.

As mentioned earlier, $\mathrm{Im}G_{zz}(1,1)$ is much less affected by the presence of the defect than $\mathrm{Im}G_{xx}(1,1)$. The local-mode amplitude, not shown in the figures, is also decreased. However, an interesting effect occurs, which can be seen in Figs. 11 and 12: $\mathrm{Im}G_{zz}(1,1)$ shows a depression or loss of amplitude around the impurity resonance frequency, in contrast to the behavior of $\mathrm{Im}G_{xx}(1,1)$. This effect begins to appear in the mass-defect case (Fig. 9) but is much stronger when force changes are also present. $\mathrm{Im}G_{zz}(1,1)$ thus shows an *antiresonance*. It seems that some amplitude or density-of-states sum rule is operating, with $\mathrm{Im}G_{zz}$ counteracting the effects of $\mathrm{Im}G_{xx}(1,1)$ and $\mathrm{Im}G_{ii}(0,0)$ to some extent.

Table VI is a summary of some of the results indicated above, including mass changes not shown in the figures. The low-frequency peak positions are indicated for $\mathrm{Im}G_{ii}(0,0)$ and $\mathrm{Im}G_{xx}(1,1)$. For $\mathrm{Im}G_{zz}(1,1)$ the positions of the maximum and minimum that define the antiresonance are given.

TABLE VI. Resonances and antiresonances in the motion of an impurity and in the motion of its nearest neighbors. Central-force-constant changes.

ϵ	$\Delta A/A$	ν_R in $\mathrm{Im}G(0,0)$ (10^{13} cps)	ν_R in $\mathrm{Im}G_{xx}(1,1)$ (10^{13} cps)	Min and max around ν_R in $\mathrm{Im}G_{zz}(1,1)$ (10^{13} cps)
−6.3017	0	0.185	0.177	0.169–0.197
−6.3017	0.3	0.161	0.155	0.147–0.171
−6.3017	0.7	0.095	0.095	0.095–0.099
−2.9983	0	0.255	0.233	0.221–0.265
−2.9983	0.3	0.219	0.207	0.191–0.227
−2.9983	0.7	0.131	0.131	0.127–0.131
−1.4233	0	0.333	...	...
−1.4233	0.3	0.285	0.267	0.243–0.283
−1.4233	0.7	0.167	0.167	0.155–0.171
−1.0363	0	0.367	...	...
−1.0363	0.3	0.313	0.303	0.271–0.303
−1.0363	0.7	0.181	0.179	0.167–0.183

The off-diagonal Green's function $\mathrm{Im}G_{xy}(1,1)$ is shown in Fig. 14 for impurities with the masses of Ag and Mn in Al. It has appreciable low-frequency structure with weakened force constants and high-frequency structure with strong forces.

It would perhaps be more physically transparent to rotate the reference coordinate system about the z axis along the line joining the impurity and neighbor (1,1,0). Then the diagonal Green's functions are $G_{x'x'}(1,1)=G_{xx}(1,1)+G_{xy}(1,1)$, $G_{y'y'}=G_{xx}-G_{xy}$, and G_{zz}, and the off-diagonal Green's functions vanish. The diagonal Green's functions, then, truly represent the square amplitude of motion of the neighbors of the impurity. The defect characteristics are then brought out more sharply and the host-lattice characteristics are suppressed. For instance, in all cases of weakened forces the $\nu=0.887\times10^{13}$-cps peak disappears in $\mathrm{Im}G_{x'x'}$ and is replaced with a structure similar to the high frequency-impurity structure. The Γ_{15} resonance is also sharpened.

V. CONCLUSION

Although we have evaluated our equations numerically for only a limited range of parameters ($-6.3<\epsilon<0$ and $-2<\Delta A/A<0.7$), there are some conclusions that can be drawn which are quite likely to hold in general:

(a) The resonance characteristics of the defect system (frequencies and amplitudes) are more sensitive to force-constant changes than to mass changes.

(b) Of all the modes that must be considered to determine the motion of the neighbors of the impurity, the Γ_{15} mode is by far the most important one. Since this is the only mode in which the impurity moves, and since the impurity is directly coupled to all the force-constant

changes, the effective disturbance for this mode is greater than for the other modes.

(c) The neighbors of the impurity share strongly in the resonances and local modes that are caused by force-constant changes to which they are directly coupled. These large resonance amplitudes occur in the planes containing the force-constant changes.

(d) In the planes that do not contain force-constant-change components, the motion of the neighbors of the impurity exhibits an antiresonance near the resonance frequency, indicating the possible existence of a density-of-states sum rule.

Some conclusions that may apply only to the cases explicitly evaluated here are the following:

(a) When mass and force changes act in the same direction (i.e., heavy mass and weak force constants), we found only one resonance mode in all cases. When they act in opposite directions, we found two resonance modes or one resonance and one local mode.

(b) In the cases considered here the changes in noncentral force constants used were too small to produce experimentally observable effects. Such effects may appear for sufficiently large changes.

From the theoretical point of view, even in the single-impurity approximation, there are several problems that have not yet been considered. For instance, there may be some relaxation of the neighbors of the impurity to new equilibrium positions, causing an effective-force-constant change *among* the neighbors in addition to the impurity-neighbors ones considered here. To our knowledge, the effects of anharmonic impurity-lattice coupling for heavy impurities has not been treated.

Experimentally, a system such as Al plus a low concentration of heavy impurities seems to be a profitable one to study via incoherent neutron scattering, because Al itself is an almost perfectly coherent scatterer.

We have studied the effect of the impurities considered here on the phonons of the Al system (e.g., shift, broadening, and branch mixing); these results will be presented in a subsequent paper.

ACKNOWLEDGMENTS

The authors are greatly indebted to Dr. L. Raubenheimer, to Dr. G. Gilat, and to other members of the Solid State Division of Oak Ridge National Laboratories for supplying the data and computer programs which were of great help in evaluating numerical results. One of the authors (K.L.) wishes to thank Dr. Samuel P. Bowen, Dr. Manuel Gomez, Dr. Hilary Jones, and Dr. William C. Kerr for many helpful discussions. Special thanks are due to Dr. Andras Lakatos for his professional advice and encouragement throughout the course of this work.

APPENDIX A

For the fcc case with force-constant changes between the impurity and its nearest neighbors (preserving the point symmetry of the cage), the irreducible representation Γ of the full cubic group appears in $V(1-g_d{}^0Q)V^{-1}$ a total of $N(\Gamma)$ times as follows[3]:

$$n(\Gamma_1)=1,\quad n(\Gamma_2)=1,\quad n(\Gamma_{12})=2,$$
$$n(\Gamma_{15}')=2,\quad n(\Gamma_{25}')=2,\quad n(\Gamma_2')=1,$$
$$n(\Gamma_{12}')=1,\quad n(\Gamma_{25})=2,\quad n(\Gamma_{15})=4.$$

Let the perfect-lattice central- and noncentral-force constants be denoted by $\alpha_0+\gamma_0$, $\alpha_0-\gamma_0$, and β_0, e.g.,[23]

$$A_{im}(1,1,0)=\begin{bmatrix}\alpha_0 & \gamma_0 & 0\\ \gamma_0 & \alpha_0 & 0\\ 0 & 0 & \beta_0\end{bmatrix}.$$

Let $\alpha\equiv\alpha_0-\alpha_{\text{new}}$, and similarly for β and γ. (When only central forces change, $\alpha=\gamma$ and $\beta=0$.) Using the notation of Table II, the resonance denominators are

$$D(\Gamma_1)=1+(\alpha+\gamma)(G_1+2G_3-2G_4+G_5-G_6-G_7-G_9-2G_{10}-4G_{12}-2G_{13}),$$
$$D(\Gamma_2)=1+(\alpha-\gamma)(G_1-2G_3+2G_4+G_5-G_6-G_7+G_9+2G_{10}-4G_{12}+2G_{13}),$$
$$D(\Gamma_{12})=1+2\alpha(G_1+G_5-G_6-G_7+2G_{12})+2\gamma(-G_3+G_4-G_9+G_{10}+G_{13})+(\alpha^2-\gamma^2)[(G_1+G_5-G_6-G_7+2G_{12})^2 -(G_3-G_4+G_9-G_{10}-G_{13})^2-3(G_3+G_4-G_{10}+G_{13})^2],$$
$$D(\Gamma_{15}')=1+\beta(G_1+2G_4-G_8+2G_{13})+(\alpha-\gamma)(G_1-G_5+G_6-G_7+G_9)+\beta(\alpha-\gamma)[(2G_4-G_8+2G_{13}) \times(-G_5+G_6-G_7+G_9)+G_1(G_1+2G_4-G_5+G_6-G_7-G_8+G_9+2G_{13})-4(G_2-G_{11}+G_{12})^2],$$
$$D(\Gamma_{25}')=1+\beta(G_1-2G_4-G_8-2G_{13})+(\alpha+\gamma)(G_1-G_5+G_6-G_7-G_9)+\beta(\alpha+\gamma)[(2G_4+G_8+2G_{13}) \times(G_5-G_6+G_7+G_9)+G_1(G_1-2G_4-G_5+G_6-G_7-G_8-G_9-2G_{13})-4(G_2-G_{11}-G_{12})^2],$$

[23] G. Leibfried, *Handbuch der Physik*, edited by S. Flügge (Springer-Verlag, Berlin, 1955), Vol. 7, Part 1.

$$D(\Gamma_2')=1+\beta(G_1-4G_4-2G_5+G_8+4G_{13}),$$
$$D(\Gamma_{12}')=1+\beta(G_1+2G_4-2G_5+G_8-2G_{13}),$$

and

$$D(\Gamma_{25})=1+2\alpha(G_1-G_3+G_4+G_7-G_{10}-G_{13})+2\gamma(G_9-2G_{12})+(\alpha^2-\gamma^2)[(G_1-G_3+G_4+G_7-G_{10}-G_{13})^2 -(G_9-2G_{12})^2-(G_3+G_4-G_5-G_6+G_{10}-G_{13})^2].$$

$D(\Gamma_{15})$ has been explicitly evaluated only for central-force-constant changes. In the general case, $D(\Gamma_{15})$ is the determinant of the matrix given below (central force change):

$$D(\Gamma_{15})=1-M_0\epsilon\omega^2G_1+2\alpha(5G_1-8G_2+G_3-9G_4+G_7+G_9+G_{10}+2G_{12}+G_{13}) -2M_0\epsilon\omega^2\alpha[G_1^2-4(G_2+G_4)^2+G_1(G_3-G_4+G_7+G_9+G_{10}+2G_{12}+G_{13})].$$

In general, $D(\Gamma_{15})$ is the determinant of the 4×4 matrix with the following elements:

$$(1,1)=1-M_0\epsilon\omega^2(G_1+8G_2+4G_3)/13,$$
$$(1,2)=20(\sqrt{91})[1-\alpha(5G_2+2G_3-G_5-G_6-G_7-2G_{10}-2G_{11})+\gamma(G_4+G_9+4G_{12})]/91,$$
$$(1,3)=-\tfrac{1}{5}(\sqrt{14})[1-\beta(4G_2+3G_3-2G_5-G_8-4G_{11})],$$
$$(1,4)=2(\sqrt{26})[\alpha(G_4+G_9+4G_{12})-\gamma(5G_2+2G_3-G_5-G_6-G_7-2G_{10}-2G_{11})]/13,$$
$$(2,1)=2(\sqrt{91})M_0\epsilon\omega^2(G_1-2G_2+G_3)/91,$$
$$(2,2)=10[1-\alpha(-5G_1+14G_2-6G_3-G_5-G_6-G_7-2G_{10}+2G_{11})-\gamma(4G_4-G_9)]/7,$$
$$(2,3)=\tfrac{1}{10}(\sqrt{26})[1-\beta(3G_1-4G_2-2G_5-G_8+4G_{11})],$$
$$(2,4)=-(\sqrt{14})[\alpha(4G_4-G_9)+\gamma(-5G_1+14G_2-6G_3-G_5-G_6-G_7-2G_{10}+2G_{11})]/7,$$
$$(3,1)=-2(\sqrt{14})M_0\epsilon\omega^2(2G_1+3G_2-5G_3)/91,$$
$$(3,2)=5(\sqrt{26})[3-\alpha(13G_1+28G_2-46G_3-3G_5-3G_6-3G_7-6G_{10}+20G_{11})-\gamma(-16G_4-3G_9+14G_{12})]/91,$$
$$(3,3)=1+\tfrac{1}{5}\beta(13G_1+6G_2-28G_3+10G_5+5G_8-6G_{11}),$$
$$(3,4)=-(\sqrt{91})[\alpha(-16G_4-3G_9+14G_{12})+\gamma(13G_1+28G_2-46G_3-3G_5-3G_6-3G_7-6G_{10}+20G_{11})]/91,$$
$$(4,1)=-2(\sqrt{26})M_0\epsilon\omega^2G_4/13,$$
$$(4,2)=5(\sqrt{14})[-\alpha(8G_4-G_9-2G_{12})+\gamma(G_1-2G_4-G_5-G_6+G_7+2G_{13})]/7,$$
$$(4,3)=\tfrac{2}{5}(\sqrt{91})\beta G_4,$$

and

$$(4,4)=1+\alpha(G_1-2G_4-G_5-G_6+G_7+2G_{13})-\gamma(8G_4-G_9-2G_{12}).$$

APPENDIX B

For the bcc case with force-constant changes between the impurity and its nearest and next-nearest neighbors, the irreducible representation Γ of the full cubic group appears in $V(1-g_d{}^0Q)V^{-1}$ a total of $n(\Gamma)$ times as follows[3]:

$$n(\Gamma_1)=2,\quad n(\Gamma_{12})=2,\quad n(\Gamma_{15}')=2,$$
$$n(\Gamma_{25}')=3,\quad n(\Gamma_2')=1,\quad n(\Gamma_{12}')=1,$$
$$n(\Gamma_{25})=2,\quad n(\Gamma_{15})=5.$$

There are now two central and two noncentral force constants,[23] denoted by $\alpha_0+2\gamma_0$, η_0, $\alpha_0-\gamma_0$, and β_0:

$$A_{im}(1,1,1)=\begin{bmatrix}\alpha_0 & \gamma_0 & \gamma_0\\ \gamma_0 & \alpha_0 & \gamma_0\\ \gamma_0 & \gamma_0 & \alpha_0\end{bmatrix},\quad A_{im}(2,0,0)=\begin{bmatrix}\eta_0 & 0 & 0\\ 0 & \beta_0 & 0\\ 0 & 0 & \beta_0\end{bmatrix}.$$

Let $\alpha\equiv\alpha_0-\alpha_{\text{new}}$, and similarly for γ, η, and β. Force-constant changes to next-nearest neighbors can be left out by letting $\eta=\beta=0$. Central-force changes correspond to $\alpha=\gamma$ and $\beta=0$. Using the notation of Table II, the resonance

denominators are

$$D(\Gamma_1)=1+2(\alpha+2\gamma)(G_1-2G_4+G_5+2G_6-G_7-2G_8-G_9+2G_{10})+2\eta(G_1+4G_6-G_{11})+4\eta(\alpha+2\gamma)$$
$$\times[-4(G_2-2G_3-G_{13}-2G_{15})^2+(G_1+4G_6-G_{11})(G_1-2G_4+G_5+2G_6-G_7-2G_8-G_9+2G_{10})],$$
$$D(\Gamma_{12})=1+2(\alpha-\gamma)(G_1-2G_4+G_5-G_6-G_7+G_8-G_9+2G_{10})+2\eta(G_1-2G_6-G_{11})+4\eta(\alpha-\gamma)$$
$$\times[-4(G_2+G_3-G_{13}+G_{15})^2+(G_1-2G_6-G_{11})(G_1-2G_4+G_5-G_6-G_7+G_8-G_9+2G_{10})],$$
$$D(\Gamma_{15}')=1+2(\alpha-\gamma)(G_1-G_5-G_6-G_7+G_8+G_9)+2\beta(G_1-2G_6-G_{12})+4\beta(\alpha-\gamma)$$
$$\times[-4(G_2+G_3-G_{14}+G_{15})^2+(G_1-2G_6-G_{12})(G_1-G_5-G_6-G_7+G_8+G_9)],$$
$$D(\Gamma_2')=1+(\alpha+2\gamma)(G_1-2G_4+G_5+2G_6+G_7+2G_8+G_9-2G_{10}),$$
$$D(\Gamma_{12}')=1+(\alpha-\gamma)(G_1-2G_4+G_5-G_6+G_7-G_8+G_9-2G_{10}),$$

and

$$D(\Gamma_{25})=1+2(\alpha-\gamma)(G_1-G_5-G_6+G_7-G_8-G_9)+2\beta(G_1-2G_5+G_{12})$$
$$+4\beta(\alpha-\gamma)[-4(2G_3-G_{15}+G_{16})^2+(G_1-2G_5+G_{12})(G_1-G_5-G_6+G_7-G_8-G_9)].$$

$D(\Gamma_{25}')$ is the determinant of the 3×3 matrix with the following elements:

$$(1,1)=1+\tfrac{1}{3}(\alpha+2\gamma)(3G_1+2G_4-G_5-2G_6-3G_7-6G_8+G_9-2G_{10}),$$
$$(1,2)=\tfrac{2}{3}(\sqrt{6})\beta(G_2-G_{14}-G_{15}-G_{16}),$$
$$(1,3)=\tfrac{2}{3}\sqrt{2}(\alpha-\gamma)(-G_4-G_5+G_6+G_9+G_{10}),$$
$$(2,1)=\tfrac{2}{3}(\sqrt{6})(\alpha+2\gamma)(G_2-G_{14}-G_{15}-G_{16}),$$
$$(2,2)=1+\beta(G_1+2G_6-G_{12}),$$
$$(2,3)=\tfrac{2}{3}\sqrt{3}(\alpha-\gamma)(G_2-3G_3-G_{14}-G_{15}+2G_{16}),$$
$$(3,1)=\tfrac{2}{3}\sqrt{2}(\alpha+2\gamma)(-G_4-G_5+G_6+G_9+G_{10}),$$
$$(3,2)=\tfrac{2}{3}\sqrt{3}\beta(G_2-3G_3-G_{14}-G_{15}+2G_{16}),$$

and

$$(3,3)=1+\tfrac{1}{3}(\alpha-\gamma)(3G_1+4G_4+G_5+5G_6-3G_7+3G_8-G_9-4G_{10}).$$

$D(\Gamma_{15})$ is the determinant of the 5×5 matrix with the following elements:

$$(1,1)=1-M_0\epsilon\omega^2G_1,$$
$$(1,2)=-(\sqrt{6})\beta(G_1-G_{10}),$$
$$(1,3)=\tfrac{2}{3}(\sqrt{3})\eta(G_1-G_9),$$
$$(1,4)=-\tfrac{2}{3}(\sqrt{6})(\alpha+2\gamma)(G_1-G_2-2G_3),$$
$$(1,5)=\tfrac{4}{3}\sqrt{3}(\alpha-\gamma)(G_1-G_2+G_3),$$
$$(2,1)=\tfrac{1}{3}(\sqrt{6})[3-M_0\epsilon\omega^2(G_9+2G_{10})],$$
$$(2,2)=1+\beta(G_1+2G_4+2G_5-2G_9-4G_{10}+G_{12}),$$
$$(2,3)=-\tfrac{1}{9}(\sqrt{2})[3+\eta(G_1+4G_4-2G_9-4G_{10}+G_{11})],$$
$$(2,4)=\tfrac{2}{3}(\alpha+2\gamma)(3G_2-2G_3-2G_9-4G_{10}+G_{13}+2G_{14}+4G_{15}+2G_{16}),$$
$$(2,5)=\tfrac{2}{3}\sqrt{2}(\alpha-\gamma)(-3G_2-G_3+2G_9+4G_{10}-G_{13}-2G_{14}+2G_{15}+G_{16}),$$
$$(3,1)=\tfrac{2}{3}\sqrt{3}M_0\epsilon\omega^2(G_9-G_{10}),$$
$$(3,2)=\tfrac{1}{2}\sqrt{2}[1+\beta(G_1-4G_4+2G_5+4G_9-4G_{10}+G_{12})],$$
$$(3,3)=\tfrac{2}{3}[1+\eta(G_1-2G_4-2G_9+2G_{10}+G_{11})],$$
$$(3,4)=\tfrac{2}{3}\sqrt{2}(\alpha+2\gamma)(2G_3+2G_9-2G_{10}-G_{13}+G_{14}-G_{15}+G_{16}),$$
$$(3,5)=\tfrac{2}{3}(\alpha-\gamma)(2G_3-4G_9+4G_{10}+2G_{13}-2G_{14}-G_{15}+G_{16}),$$
$$(4,1)=-\tfrac{2}{3}(\sqrt{6})M_0\epsilon\omega^2(G_2+2G_3),$$
$$(4,2)=-2\beta(G_2+4G_3-G_{14}-G_{15}-G_{16}),$$
$$(4,3)=\tfrac{2}{3}\sqrt{2}\eta(G_2+6G_3-G_{13}-2G_{15}),$$

$$(4,4)=1+\tfrac{1}{3}(\alpha+2\gamma)(3G_1-8G_2-16G_3+2G_4-G_5-2G_6+3G_7+6G_8-G_9+2G_{10}),$$
$$(4,5)=\tfrac{2}{3}\sqrt{2}(\alpha-\gamma)(4G_2+8G_3-G_4-G_5+G_6-G_9-G_{10}),$$
$$(5,1)=\tfrac{4}{3}\sqrt{3}M_0\epsilon\omega^2(G_2-G_3),$$
$$(5,2)=\sqrt{2}\beta(2G_2-4G_3-2G_{14}+G_{15}+G_{16}),$$
$$(5,3)=-\tfrac{4}{3}\eta(G_2-3G_3-G_{13}+G_{15}),$$
$$(5,4)=\tfrac{2}{3}\sqrt{2}(\alpha+2\gamma)(4G_2-4G_3-G_4-G_5+G_6-G_9-G_{10}),$$

and

$$(5,5)=1+\tfrac{1}{3}(\alpha-\gamma)(3G_1-16G_2+16G_3+4G_4+G_5+5G_6+3G_7-3G_8+G_9+4G_{10}).$$

APPENDIX C

The Green's functions for the nearest neighbors of the impurity with central-force-constant changes in the fcc case have been worked out up to a point that makes computer evaluation very easy. The expressions below could be simplified further at the expense of much work and little gain. We first define a large list of symbols for quantities that enter in the Green's functions; the latter are given at the end of this Appendix. Some of the symbols used here are defined in Table II and in Appendix A.

Let

$$\chi_1=(\sqrt{13})M_0\epsilon\omega^2/13, \qquad \chi_2=-2(\sqrt{7})(M_0\epsilon\omega^2-10\alpha)/7,$$
$$\chi_3=2(\sqrt{182})(2M_0\epsilon\omega^2-13\alpha)/91, \qquad \chi_4=2\sqrt{2}\alpha,$$
$$\chi_5=-5(\sqrt{7})\alpha/14, \qquad \chi_6=(\sqrt{182})\alpha/28, \qquad \text{and} \quad \chi_7=-\tfrac{1}{4}\sqrt{2}\alpha;$$

$$t_1=(\sqrt{13})\{1+4M_0\epsilon\omega^2(2G_2+G_3)-2\alpha(-5G_1+28G_2+7G_3+5G_4-4G_5-4G_6-5G_7-5G_9-9G_{10}-8G_{11}-18G_{12}-G_{13})$$
$$-8M_0\epsilon\omega^2\alpha[G_1(-G_2-G_3+G_4)+G_2(2G_2+4G_4+G_5+G_6-G_7-G_9+2G_{11}-2G_{13})$$
$$+G_3(-G_3+3G_4-G_7-G_9-G_{10}-2G_{12}-G_{13})+G_4(G_5+G_6+G_7+G_9+2G_{10}+2G_{11}+4G_{12})]\}/13,$$

$$p_1=-2(\sqrt{7})\{1+M_0\epsilon\omega^2(-2G_2+G_3)+2\alpha(6G_2-5G_3-5G_4-G_5-G_6-G_{10}+2G_{11}+2G_{12}+G_{13})$$
$$-2M_0\epsilon\omega^2\alpha[G_1(G_2-G_3-G_4)+G_2(2G_2-G_5-G_6+G_7+G_9+2G_{11}+4G_{12}+2G_{13})$$
$$-G_3(G_3+G_4+G_7+G_9+G_{10}+2G_{12}+G_{13})-G_4(G_5+G_6+G_7+G_9+2G_{10}-2G_{11})]\}/7,$$

$$q_1=2(\sqrt{182})\{2+M_0\epsilon\omega^2(3G_2-5G_3)-\alpha(-7G_1+60G_2-50G_3+20G_4-3G_5-3G_6-7G_7-7G_9-10G_{10}$$
$$+20G_{11}+6G_{12}-4G_{13})-M_0\epsilon\omega^2\alpha[G_1(-3G_2+10G_3+3G_4)+G_2(-20G_2-14G_4+3G_5$$
$$+3G_6-3G_7-3G_9-20G_{11}-26G_{12}-6G_{13})+G_3(10G_3-4G_4+10G_7+10G_9+10G_{10}+20G_{12}+10G_{13})$$
$$+G_4(3G_5+3G_6+3G_7+3G_9+6G_{10}-20G_{11}-14G_{12})]\}/91,$$

$$r_1=2\sqrt{2}\{59M_0\epsilon\omega^2G_4-91\alpha(-G_1+10G_4+G_5+G_6-G_7-G_9-2G_{12}-2G_{13})-M_0\epsilon\omega^2\alpha[G_1(11G_2+80G_3-11G_4)$$
$$+G_2(-342G_4-11G_5-11G_6+11G_7+11G_9+22G_{12}+22G_{13})+G_3(-182G_4-80G_5-80G_6+80G_7+80G_9$$
$$+160G_{12}+160G_{13})-G_4(11G_5+11G_6+11G_7+11G_9+22G_{10}+320G_{11}+342G_{12})]\}/91,$$

$$t_2=(\sqrt{13})\{1-M_0\epsilon\omega^2G_1-\alpha(-10G_1+11G_2-4G_3+19G_4+G_5+G_6-G_7-G_9+2G_{11}-2G_{13})$$
$$-M_0\epsilon\omega^2\alpha[G_1(G_1-2G_2-2G_4-G_5-G_6+G_7+G_9-2G_{11}+2G_{13})+4(G_2+G_4)(G_3-2G_4)]\}/13,$$

$$p_2=(\sqrt{7})\{1-M_0\epsilon\omega^2G_1-\alpha(-5G_1+2G_2+4G_3+14G_4+G_5+G_6-G_7-G_9-2G_{11}-4G_{12}-2G_{13})-M_0\epsilon\omega^2\alpha$$
$$\times[G_1(G_1+2G_2-2G_4-G_5-G_6+G_7+G_9+2G_{11}+4G_{12}+2G_{13})-4(G_2+G_4)(G_3+2G_4)]\}/14,$$

$$q_2=(\sqrt{182})\{3-3M_0\epsilon\omega^2G_1-\alpha(-43G_1+20G_2+40G_3+70G_4+3G_5+3G_6-3G_7-3G_9-20G_{11}-26G_{12}-6G_{13})$$
$$-M_0\epsilon\omega^2\alpha[G_1(3G_1+20G_2-6G_4-3G_5-3G_6+3G_7+3G_9+20G_{11}+26G_{12}+6G_{13})-(G_2+G_4)(40G_3+24G_4)]\}/364,$$

$$r_2=\sqrt{2}\{-48M_0\epsilon\omega^2G_4-91\alpha(G_1-10G_4-G_5-G_6+G_7+G_9+2G_{12}+2G_{13})-M_0\epsilon\omega^2\alpha[(11G_1+80G_3)$$
$$\times(-G_1+2G_4+G_5+G_6-G_7-G_9-2G_{12}-2G_{13})+408G_2G_4+320G_4(G_{11}+G_{12})+88G_4^2]\}/364,$$

$$t_3=(\sqrt{13})\{\alpha(5G_2+2G_3-G_4-G_5-G_6-G_7-G_9-2G_{10}-2G_{11}-4G_{12})-M_0\epsilon\omega^2\alpha$$
$$\times[-G_1(G_1+2G_2+2G_3+G_5+G_6+G_7+G_9+2G_{10}+2G_{11}+4G_{12})+(8G_2+4G_3)(G_2+G_4)]\}/13,$$

$$p_3=(\sqrt{7})\{\alpha(-5G_1+14G_2-6G_3+4G_4-G_5-G_6-G_7-G_9-2G_{10}+2G_{11})-M_0\epsilon\omega^2\alpha$$
$$\times[-G_1(G_1-2G_2+2G_3+G_5+G_6+G_7+G_9+2G_{10}-2G_{11})+4(2G_2-G_3)(G_2+G_4)]\}/14,$$

$$q_3=(\sqrt{182})\{\alpha(13G_1+28G_2-46G_3-16G_4-3G_5-3G_6-3G_7-3G_9-6G_{10}+20G_{11}+14G_{12})-M_0\epsilon\omega^2\alpha$$
$$\times[G_1(-3G_1+20G_2-6G_3-3G_5-3G_6-3G_7-3G_9-6G_{10}+20G_{11}+14G_{12})+8(3G_2-5G_3)(G_2+G_4)]\}/364,$$
$$r_3=\sqrt{2}\{91-M_0\epsilon\omega^2(59G_1-48G_2+80G_3)-91\alpha(-9G_1+16G_2-2G_3+8G_4-G_5-G_6-G_7-G_9-2G_{10}-2G_{12})$$
$$-M_0\epsilon\omega^2\alpha[G_1(11G_1+320G_2+102G_3+11G_5+11G_6+11G_7+11G_9+22G_{10}+320G_{11}+342G_{12})$$
$$-G_2(408G_2+640G_3+88G_4+320G_{11}+320G_{12})+80G_3(2G_3-8G_4+G_5+G_6+G_7+G_9+2G_{10}+2G_{12})]\}/364,$$
$$t_4=(\sqrt{13})\{1-M_0\epsilon\omega^2G_1-2\alpha(-5G_1+8G_2-G_3+9G_4-G_7-G_9-G_{10}-2G_{12}-G_{13})$$
$$-2M_0\epsilon\omega^2\alpha[G_1(G_1+G_3-G_4+G_7+G_9+G_{10}+2G_{12}+G_{13})-4(G_2+G_4)^2]\}/13,$$
$$p_4=-(\sqrt{91})t_4/14,$$
$$q_4=-5(\sqrt{14})t_4/14,$$

and

$$r_4=40\sqrt{2}\{M_0\epsilon\omega^2G_4-M_0\epsilon\omega^2\alpha[G_1(-G_1+G_2+G_4+G_5+G_6-G_7-G_9-2G_{12}-2G_{13})$$
$$+G_2(6G_4-G_5-G_6+G_7+G_9+2G_{12}+2G_{13})+G_4(-2G_3+8G_4-G_5-G_6-G_7-G_9-2G_{10}-2G_{12})]\}/91;$$
$$Y_1=[\chi_1t_1+\chi_2p_1+\chi_3q_1+\chi_4r_1]/D(\Gamma_{15}),$$
$$Y_2=[\chi_1t_2+\chi_2p_2+\chi_3q_2+\chi_4r_2]/D(\Gamma_{15}),$$
$$Y_3=[\chi_1t_3+\chi_2p_3+\chi_3q_3+\chi_4r_3]/D(\Gamma_{15}),$$
$$Y_4=[\chi_1t_4+\chi_2p_4+\chi_3q_4+\chi_4r_4]/D(\Gamma_{15}),$$
$$Y_5=[\chi_5p_1+\chi_6q_1+\chi_7r_1]/D(\Gamma_{15}),$$
$$Y_6=-\tfrac{1}{12}\alpha[1/D(\Gamma_1)+2/D(\Gamma_{12})+3/D(\Gamma_{25}')+3/D(\Gamma_{25})]+[\chi_5(p_2+p_3)+\chi_6(q_2+q_3)+\chi_7(r_2+r_3)]/D(\Gamma_{15}),$$
$$Y_7=\alpha[-2/D(\Gamma_1)+2/D(\Gamma_{12})+3/D(\Gamma_{25})]/24+[\chi_5p_2+\chi_6q_2+\chi_7r_2]/D(\Gamma_{15}),$$
$$Y_8=[\chi_5p_4+\chi_6q_4+\chi_7r_4]/D(\Gamma_{15}),$$
$$Y_9=\alpha[-2/D(\Gamma_1)+2/D(\Gamma_{12})+3/D(\Gamma_{25})]/24+[\chi_5p_3+\chi_6q_3+\chi_7r_3]/D(\Gamma_{15}),$$
$$Y_{10}=\tfrac{1}{12}\alpha[-1/D(\Gamma_1)-2/D(\Gamma_{12})+3/D(\Gamma_{25}')]+[\chi_5(p_2-p_3)+\chi_6(q_2-q_3)+\chi_7(r_2-r_3)]/D(\Gamma_{15}),$$
$$Y_{11}=\tfrac{1}{12}\alpha[1/D(\Gamma_1)+2/D(\Gamma_{12})-3/D(\Gamma_{25}')]+[\chi_5(p_2-p_3)+\chi_6(q_2-q_3)+\chi_7(r_2-r_3)]/D(\Gamma_{15}),$$
$$Y_{12}=\alpha[2/D(\Gamma_1)-2D(\Gamma_{12})+3/D(\Gamma_{25})]/24+[\chi_5p_2+\chi_6q_2+\chi_7r_2]/D(\Gamma_{15}),$$
$$Y_{13}=\alpha[-2/D(\Gamma_1)+2/D(\Gamma_{12})-3/D(\Gamma_{25})]/24-[\chi_5p_3+\chi_6q_3+\chi_7r_3]/D(\Gamma_{15}),$$

and

$$Y_{14}=\tfrac{1}{12}\alpha[1/D(\Gamma_1)+2/D(\Gamma_{12})+3/D(\Gamma_{25}')-3/D(\Gamma_{25})]+[\chi_5(p_2+p_2)+\chi_6(q_2+q_3)+\chi_7(r_2+r_3)]/D(\Gamma_{15});$$

and

$$Z_1=Y_1G_2+Y_2(G_1+2G_3+G_5+G_6+G_7+2G_{10})+Y_3(G_9+2G_{12})+2Y_4(G_2+G_{11}),$$
$$Z_2=Y_1G_4+Y_2(G_9+2G_{12})+Y_3(G_1-2G_4-G_5-G_6+G_7+2G_{13})+2Y_4G_{12},$$
$$Z_3=Y_1G_3+4Y_2(G_2+G_{11})+4Y_3G_{12}+Y_4(G_1+2G_5+G_8),$$
$$Z_4=Y_5(G_2+G_4)+Y_6G_1+2Y_7G_3+2Y_8(G_2+G_{11}+G_{12})-2Y_9G_4+Y_{10}G_5+Y_{11}G_6$$
$$+2Y_{12}(G_{10}+G_{12})-2Y_{13}(G_{12}+G_{13})+Y_{14}(G_7+G_9),$$
$$Z_5=Y_5G_2+Y_6G_3+Y_7(G_1-G_4+G_5-G_{13})+2Y_8(G_2+G_{11})-Y_9G_{12}+Y_{10}(G_3-G_{12})+Y_{11}G_{10}$$
$$+Y_{12}(G_4+G_6+G_7+G_{13})-Y_{13}(G_9+G_{12})+Y_{14}(G_{10}+G_{12}),$$
$$Z_6=(Y_5-Y_6+Y_{11})G_4+Y_9(G_1+G_3-G_6-G_{10})-(Y_7-2Y_8-Y_{11}-Y_{12}-Y_{14})G_{12}$$
$$+Y_{12}G_9+Y_{13}(G_3+G_5-G_7-G_{10})-(Y_{10}-Y_{14})G_{13},$$
$$Z_7=Y_5G_3+(Y_6+Y_7+Y_{11}+Y_{12})G_2+(Y_7+Y_{10}+Y_{12}+Y_{14})G_{11}+Y_8(G_1+2G_5+G_8)+(Y_9-Y_{11}-Y_{13}+Y_{14})G_{12},$$
$$Z_8=Y_5(G_2-G_4)+Y_6G_5+2Y_7(G_3-G_{12})+2Y_8(G_2+G_{11}-G_{12})-2Y_9G_{13}+Y_{10}(G_1-G_9)$$
$$+Y_{11}G_7+2Y_{12}G_{10}-2Y_{13}(G_4+G_{12})+Y_{14}G_6,$$
$$Z_9=-Y_5(G_2-G_4)-Y_6G_6-2Y_7G_{10}-2Y_8(G_2+G_{11}-G_{12})-2Y_9(G_4+G_{12})$$
$$-Y_{10}G_7-Y_{11}(G_1-G_9)-2Y_{12}(G_3-G_{12})-2Y_{13}G_{13}-Y_{14}G_5,$$
$$Z_{10}=(Y_5+Y_{10}-Y_{14})G_4+Y_6(G_{12}+G_{13})+(Y_7+2Y_8+Y_{10}-Y_{12})G_{12}+Y_9(-G_3-G_5+G_7+G_{10})-Y_{11}G_{13}$$
$$-Y_{13}(G_1+G_3-G_6-G_{10}),$$

$$Z_{11}=Y_5G_2+(Y_6+Y_9-Y_{11}+Y_{13})G_{12}+(Y_6+Y_{10})G_{10}+Y_7(G_4+G_6+G_7+G_{13})+2Y_8(G_2+G_{11})+Y_9G_9 +(Y_{11}+Y_{14})G_3+Y_{12}(G_1-G_4+G_5-G_{13}),$$

$$Z_{12}=-Y_5G_3-(Y_6+Y_7+Y_{11}+Y_{12})G_{11}-(Y_6+Y_9-Y_{13})G_{12}-(Y_7+Y_{10}+Y_{12}+Y_{14})G_2-Y_8(G_1+2G_5+G_8),$$

and

$$Z_{13}=Y_5(G_2+G_4)+Y_6(G_7+G_9)+2Y_7(G_{10}+G_{12})+2Y_8(G_2+G_{11}+G_{12})+2Y_9(G_{12}+G_{13})+Y_{10}G_6 +Y_{11}G_5+2Y_{12}G_3+2Y_{13}G_4+Y_{14}G_1.$$

The Green's functions are then given by

$$G_{xx}(1,1;\omega)=G_1(1+Z_4)+G_2Z_1+2G_3Z_5+G_4(Z_2-2Z_6)+G_5Z_8-G_6Z_9 +(G_7+G_9)Z_{13}+2(G_{10}+G_{12})Z_{11}+2(G_{12}+G_{13})Z_{10},$$

$$G_{zz}(1,1;\omega)=G_1+4G_2Z_7+G_3Z_3-4(G_{11}+G_{12})Z_{12},$$

and

$$G_{xy}(1,1;\omega)=G_1Z_4+G_2Z_2+2G_3Z_6+G_4(Z_1-2Z_5)+G_5Z_9-G_6Z_8+(G_7+G_9)Z_{13}+2(G_{10}+G_{12})Z_{10}+2(G_{12}+G_{13})Z_{11}.$$

PHYSICAL REVIEW VOLUME 175, NUMBER 3 15 NOVEMBER 1968

Landau Fermi-Liquid Parameters in Na and K

T. M. RICE
Bell Telephone Laboratories, Murray Hill, New Jersey 07971
(Received 14 June 1968)

Theoretical estimates are presented for the Landau Fermi-liquid parameters in Na and K, and a comparison is made with the experimental values. The calculations are presented in two parts. The effects of the Coulomb interaction between the electrons are taken from previous calculations which use the random-phase approximation and include exchange diagrams approximately. The electron-phonon-interaction effects are calculated using the observed phonon spectra and a screened pseudopotential approximation for the electron-ion coupling. The theoretical estimates for Na are found to be in surprisingly good agreement with six independent experimentally determined parameters. In K, the experimental values are less accurate, but a preliminary comparison is encouraging.

I. INTRODUCTION

THE Landau theory of a Fermi liquid[1] as extended by Silin[2] has been very successful in explaining the qualitative nature of many-body effects in metals. In this theory the effects of the interactions are characterized by an effective mass m^* and an interaction function $f(\mathbf{k}\sigma,\mathbf{k}'\sigma')$ which are to be determined from experiment. Until recently, however, the experimental information on the size of f was very limited. The observation of spin waves[3,4] and high-frequency plasmalike waves[5–7] in Na and K has led to the determination of several of the Legendre coefficients of the function f. In this paper we will be concerned with a comparison of the experimental values of these coefficients, the Landau parameters, with theoretical estimates based on microscopic theory.

In metals there are two sources of interactions between electrons, (a) the Coulomb repulsion between two electrons and (b) the attraction caused by the virtual exchange of phonons. There are, in addition, effects due to the periodic potential of the ions. Na and K have Fermi surfaces which deviate from the free-electron sphere by less than 0.2%,[8] so that we will, for the most part, ignore band-structure effects. The contribution to interaction effects from the Coulomb repulsion, which we will refer to as the electron-electron contribution, may then be obtained from calculations for a uniform electron gas.[9] The derivation of the

[1] L. D. Landau, Zh. Eksperim. i Teor. Fiz. **30**, 1058 (1956) [English transl.: Soviet Phys.—JETP **3**, 920 (1956)].
[2] V. P. Silin, Zh. Eksperim. i Teor. Fiz. **33**, 495 (1957) [English transl.: Soviet Phys.—JETP **6**, 945 (1958)].
[3] P. M. Platzman and P. A. Wolff, Phys. Rev. Letters **18**, 280 (1967).
[4] S. Schultz and G. Dunifer, Phys. Rev. Letters **18**, 283 (1967).
[5] W. M. Walsh, Jr. and P. M. Platzman, Phys. Rev. Letters **15**, 784 (1965).
[6] P. M. Platzman and W. M. Walsh, Jr., Phys Rev. Letters **19**, 514 (1967); **20**, 89(E) (1968).
[7] P. M. Platzman, W. M. Walsh, Jr., and E-Ni Foo, Phys. Rev. **172**, 689 (1968).
[8] For Na, M. J. G. Lee, Proc. Roy. Soc. (London) **A295**, 440 (1966); for K, M. J. G. Lee and L. M. Falicov, *ibid.* **A314**, 319 (1968).
[9] A. W. Overhauser [Phys. Rev. **128**, 1437 (1962); **167**, 691 (1968)] has suggested that at low temperatures K may not be a normal metal. Our calculations and the interpretation of the experimental data, which we shall cite, are based on the assumption that Na and K are normal metals.